ASTRONOMY & ASTROPHYSICS
SUPPLEMENT SERIES

*Astron. Astrophys. Suppl. Ser.* **99**, 407-435 (1993)



# Polarization in low luminosity radio galaxies

A. Capetti[1], R. Morganti[2], P. Parma[2] and R. Fanti[2,3]

[1] Istituto di Fisica Generale, via Giuria 1,10125 Torino, Italy
[2] Istituto di Radio Astronomia, Via Irnerio, 46, 40126 Bologna, Italy
[3] Dipartimento di Fisica, Università di Bologna, Via Irnerio 46, 40126 Bologna, Italy

Received January 28; accepted September 28, 1992

**Abstract.** — Polarization data are presented for 69 B2 radiogalaxies. The sources were observed at 20 cm in different configurations of the VLA. The results are given as integrated and mean component parameter and are compared with those from similar studies. We also present maps of total intensity with superimposed vectors representing the fractional polarization and position angle for the most interesting sources. Information on individual sources are given when interesting structures are present.

**Key words:** radio continuum: galaxies — galaxies: general — polarization

## 1. Introduction

The most recent work done on the sample of B2 low luminosity radio galaxies is the systematic observation of all objects at 1.4 GHz with different configurations of the Very Large Array (VLA). The source sample contains about one hundred objects and was obtained from the identification of B2 radio sources with bright elliptical galaxies (see Colla et al. 1975; Fanti et al. 1978). The sample was observed at the VLA at 1.4 GHz using three different configurations with a resolution ranging from 1" and 12" for the very extended sources. The VLA observations are described in a series of papers (Fanti et al. 1987 (Paper IV) and references therein). Five B2 radio galaxies were also observed at 5 GHz (Morganti et al. 1987) for a detailed study of their spectral and polarization properties. The large body of data thus obtained permitted a detailed analysis of the jet properties (Parma et al. 1987, Bicknell et al. 1990) and a more general discussion on the properties of low power radio galaxies (de Ruiter et al. 1990). The goals of these studies were to identify the factors that influence the structure of a radio source and to provide constraints on physical models of radio sources.

Polarization properties were not included in previous discussions. Polarization has become an important topic since the work of Laing (1988) and Garrington et al. (1988) on powerful radio sources: according to Laing (1988) the observed asymmetry in depolarization can be linked to relativistic beaming of the jet. More recent results on a bigger sample have been presented in two different papers by Garrington et al. (1991) and Garrington & Conway (1991). From a study of 47 double radio sources with one sided jets they found a strong asymmetry in the degree of polarization between 6 cm and 20 cm which they interpret as being due to a halo of hot gas surrounding the radio source. If the visible jet is on the near side of the source, as required by the relativistic beaming hypothesis, it will be seen through less depolarizing gas. At this point it becomes interesting to study also the polarization behavior of low luminosity radio galaxies. The properties of this class of sources are quite different from the powerful radio sources (see e.g. de Ruiter et al. 1990). Jets are very common and generally they can be adequately described by Bicknell's model (see Bicknell et al. 1990), which requires jet velocities between 1000 - 10000 km $s^{-1}$.

Since data at 20 cm are available for almost the entire sample of low luminosity radio galaxies we decided to analyze the polarization at this frequency and add new 6 cm data, in order to determine the depolarization data and compare them with the results of Garrington et al. (1988). Polarization data for the whole sample are presented here, while a discussion of the results is the object of a forthcoming paper (Parma et al. 1993). The reduction of new 6 cm data for 16 sources is presently in progress.

In Sect. 2 we discuss the observations and the data reduction procedure while in Sect. 3 we present the results in the form of radio contour plots and tables of the relevant

*Send offprint requests to*: A. Capetti, Space Telescope Science Institute, 3700, S. Martin Drive, Baltimore, MD 21218, U.S.A.

radio parameters. Comments on a number of sources are given in Sect. 4.

In Sect. 5 we compare our results with those of Garrington et al. (1988), Jägers (1986) and Strom & Jägers (1988).

## 2. Observations and data reduction

A description of the VLA and its modes of operation can be found in Napier et al. (1983).

The sample contains one hundred and three objects. Eighteen sources were already observed and studied by other authors and the references to these previous works are summarized in Paper IV. In addition to these data, seven sources for which low resolution maps were not available (see "Comments on the individual sources") have been recently reobserved at 1.4 GHz with the C configuration of the VLA. For these objects, we will present here the new maps of total intensity and polarization: more details on the sources will be given in a forthcoming paper (Parma et al. 1993).

All remaining sources were observed at 20 cm with the VLA in different configurations. Depending on the VLA configuration each source was observed for a time ranging from $\sim 10$ to $\sim 40$ minutes, at 1435 or 1465 MHz with a bandwidth of 25 or 50 MHz. For most of the sample also 1615 MHz data exist. We refer to Paper IV and references therein for further details on the observations and data reduction procedure.

The flux densities were brought on the scale of Baars et al. (1977) using 3C 286 and 3C 48 as primary flux calibrators. Polarization angles were measured relative to those of 3C 286 and 3C 138; since we did not have a secondary calibrator observed at a sufficient number of different parallactic angles (in order to determine a good solution for the instrumental polarization calibration), the data were not corrected for it. By checking (in a different set of data) the difference in fractional polarization in a number of sources for which the instrumental polarization calibration was possible, we have been able to estimate that the error is $\sim 1\%$.

Post-calibration reduction was done using the National Radio Astronomy Observatory (NRAO) AIPS package at the University of Torino and at the Istituto di Radioastronomia di Bologna.

Maps of the Stokes parameters $I$, $Q$ and $U$ were produced for each source; then maps of the polarized flux density $p = (Q^2 + U^2)^{1/2}$ and position angle $A = 0.5$ arctan $(U/Q)$ were produced from the $Q$ and $U$-maps.

The noise in the final $U$ and $Q$ maps is between 0.04 and 0.10 mJy.

Integrated values of $I$, $Q$, $U$ were computed for each source component, using only points in the $I$ maps with a signal to noise ratio $> 5\sigma_I$. From the integrals $\sum Q$ and $\sum U$ for each component we have computed

$$m = \left(\left(\sum Q\right)^2 + \left(\sum U\right)^2\right)^{1/2} / \sum I$$

and the associate position angle

$$A = 0.5 \arctan\left(\sum U\right) / \left(\sum Q\right)$$

We have also derived the mean fractional polarization

$$m' = \sum p / \sum I$$

for each component. The errors in fractional polarization and position angle have been estimated as follow: the rms error due to the thermal noise is

$$\sigma_m(\text{noise}) = N^{1/2}\, \sigma_p / \sum I$$

$$\sigma_A(\text{noise}) = 0.5\, N^{1/2}\, \sigma_p / \sum p$$

where $N$ is the number of independent points in the component and $\sigma_p$ is the noise in the $Q$ and $U$ maps; the noise in $I$ is small and can be ignored. Including the systematic error relative to instrumental polarization $\sigma_{\text{instrum}}$, the overall error is

$$\sigma_m = \left(\sigma_m^2(\text{noise}) + \sigma_{\text{instrum}}^2\right)^{1/2}$$

For the position angle we have taken into account that the uncertainty due to the instrumental polarization reflects as an additional error in position angle as:

$$\sigma_{A'} = 0.5\,(\sigma_{\text{instrum}}/m)$$

The final error is

$$\sigma_A = \left(\sigma_A^2(\text{noise}) + \sigma_{A'}^2\right)^{1/2}$$

Components are considered unpolarized if $\sum p < 5\sigma_p$ or if $m < 1\%$.

## 3. Results

We have produced polarization maps for the whole sample. Images of the most polarized sources are given in Fig. 1 in the form of contour plots of the resulting total intensity maps with superimposed vectors representing the polarization position angle (E vector) and length proportional to the amount of fractional polarization.

The value of the contour levels is always expressed in mJy/beam; polarization vectors are not shown when $I < 5\sigma_I$ or $p < 3\sigma_p$. Fractional polarization $m$, position angle $A$ and mean fractional polarization $m'$ and relative

errors, for the sources and, when possible and reliable, also for their individual components are given in Table 1. In the case of a few objects a comment is given in Sect. 4.

Some sources were excluded from the polarization study for different reasons: ten are point sources; in our observation the source 1101+38 is a point source, but extended emission was detected in another map at lower resolution (Machalsky & Condon 1985); two sources (1610+29, 1113+24) and the extended emission of the source 0331+39 are too weak for a useful study of their polarization; the source (0924+30) is too extended to be observed using the VLA and the source 1736+32 is the super-imposition of two the different objects. Therefore the final sample is formed by 69 sources.

## 4. Comments on individual sources

### 0755+37

The radio source is very polarized in general, but especially the bright inner part, with polarization values up to 30% and a quite uniform polarization angle. Another region of high polarization is the outer edge of the lobes with polarization values of 25% while in the rest of the source it remains at the level of 5%. The bright jet points to the more polarized lobe.

### 0828+32

The polarized structure is very clumpy, with polarization varying from 8% to 45%. The most polarized regions are the hot-spot regions and the outer edges of the lobes. See Parma et al. (1985) for a determination of the rotation measure.

### 0836+29

The only region of significant polarization is the south lobe where we found polarization values up to 25%. The bright jet points to the less polarized lobe.

### 0844+31

The map shown here is obtained using the new C configuration data; these low resolution data makes the extended structure visible.

### 0915+32

The polarization distribution is quite asymmetrical with the more extended south lobe being the more polarized. The polarization ratio between the two components is 2.5 while the double jet structure is very symmetric.

### 1102+30

Both lobes are very polarized with values ranging from 6% to 18%. Again the more polarized regions are the inner bright parts of the lobes and the outer edges.

### 1108+27

The presented map is obtained combining the B array and the new C array data. The addition of the low resolution data makes the extended structure now more visible and in particular the counter-jet is now well evident.

### 1116+28

A clumpy polarization structure is superposed on a smooth jet, with values varying from 6% to 13%.

### 1122+39

The presented map is obtained combining the B array and the new C array data. The structure has remained essentially the same than in the previous published map, i.e. a double "naked" jet.

### 1316+29

The polarization is larger along the spiral-like ridge visible in total intensity; we found values of about 20%. See also Condon & Mitchell (1984).

### 1322+36

The brighter jet points to the more polarized lobe.

### 1358+30

This is a large size double source (10.5') which was not recognized as such in previous papers of this series. The northern component was identified with a bright galaxy located close to its eastern edge. Now the correct identification is with a galaxy of 17 magn., whose position is marked by a 1 mJy core at RA=13 58 29.12, Dec=30 33 46.7. The galaxy has no measured red-shift. The source linear size is very likely $\gg$1 Mpc.

### 1441+26

This source is quite asymmetric in polarization, the east lobe being three times more polarized than the west lobe. No jet is visible on either side.

### 1521+28

We find a high asymmetry in polarization between the south lobe, larger and more polarized (15.5%), and the smaller north lobe (3.6%). The bright jet is the southern one, on the same side where the polarization is larger.

### 1553+24

The map shown here is obtained using the new C configuration data. The source is asymmetric with the North-West jet showing an extended low brightness lobe in agreement with the map presented by Stoke & Burns (1987).

### 1615+32

The source is quite polarized, with values from 4% to 16%, with the maximum of polarization at the outer edges of the lobes. See also Miller (1985) for another polarization study of the source.

### 1638+32

The presented map is obtained combining the B array and the new C array data. The source remains essentially the same as in the previously published map with some more extended structure.

### 1747+30

The presented map is obtained combining the B array and the new C array data. The low resolution observation confirms the asymmetry of the source. Only one lobe is present (south) while on the other side (north) a one-sided well collimated jet with no extended structure is evident.

### 1752+32

The map shown here is obtained using the new C configuration data. This low resolution observation shows that the source can not be classified anymore as a "naked" jet but as "normal" FRI double source with jets and lobe.

### 2116+26

The presented map is obtained combining the B array and the new C array data. The structure of the source remains the same with no evidence of extended low brightness lobe.

## 5. Conclusions

a) We have measured integrated ($m$) and mean ($m'$) polarization parameters for a sample of 69 B2 radiogalaxies of low luminosity and low red-shift. The distributions of $m$ and $m'$, integrated over each source, are shown in Figs. 2a and 2b. The median values are $\langle m \rangle = 3.2(+0.5/-0.33)$ and $\langle m' \rangle = 8.6(+0.81/-0.72)$. When only the sources with a double lobed structure are considered, the median over the lobes became $4.6(+0.47/-0.45)$ and $10.3(+1.28/-0.74)$ respectively (see Figs. 2c and 2d for their distribution).

Our $m$ parameter distribution (Fig. 2a) is consistent with those found, at 20 cm, in other sample of extragalactic radio sources (e.g. Conway & Strom 1985, Strom & Jägers 1988) and, for what concerns the double sources, with the Garrington et al. (1988) sample, when their sources are restricted at a comparable range in $z$(i.e. $z < 1.0$).

b) As noted in Sect. 4, in several sources we find that the more polarized lobe is the one on the side of the brighter jet. This remind us of the Laing-Garrington effect (Laing 1988, Garrington et al. 1988, 1991) and therefore suggests its existence also in sample of low luminosity/low red-shift radio galaxies. This point will be discussed in detail in a forthcoming paper (Parma et al. 1993).

*Acknowledgements.* The National Radio Astronomy Observatory is operated by Associated Universities, Inc., under contract with the National Science Foundation.

## References

Baars J.W.M., Genzel R., Pauliny-Toth I.I.K., Witzel A. 1977, A&AS 61, 99
Bicknell G.V., de Ruiter H.R., Fanti R., Morganti R., Parma P. 1990, ApJ 354, 98
Colla G., Fanti C., Fanti R., Gioia I., Lari C., Lequeux J., Lucas R., Ulrich M.H. 1975, A&AS 20, 1
Condon J.J., Mitchell K.J. 1984, ApJ 276, 472
Conway R.G., Strom R.G. 1985, AAS 61, 547
de Ruiter H.R., Parma P., Fanti C., Fanti R. 1990, A&A 227, 351
Fanti R., Gioia I., Lari C., Ulrich M.H. 1978, A&AS 34, 341
Fanti C., Fanti R., de Ruiter H.R., Parma P. 1987, A&AS 69, 57 (Paper IV)
Garrington S.T., Leahy J.P., Conway R.G., Laing R.A. 1988, Nat 331, 147
Garrington S.T., Conway R.G., Leahy J.P. 1991, MNRAS 250, 171
Garrington S.T., Conway R.G. 1991, MNRAS 250, 198
Jägers W.J. 1986, Ph.D. Thesis, Leiden
Laing R.A. 1988, Nat 331, 149
Machalsky J., Condon J.J. 1985, AJ, 90, 5
Miller L. 1985, MNRAS 215, 773.
Morganti R., Fanti C., Fanti R., Parma P., de Ruiter H.R. 1987, A&A 183, 203
Napier P.J., Thompson A.R., Ekers R.D. 1983, Proc. IEEE, 71, 1295
Parma P., Ekers R.D., Fanti R. 1985, A&AS 59, 511
Parma P., Fanti C., Fanti R., Morganti R., de Ruiter H.R. 1987, A&A 181, 244
Parma P., Morganti R., Capetti A., Fanti R., de Ruiter H.R. 1993, A&A in press
Stocke J.T., Burns J.O. 1987, ApJ 319, 671
Strom R.G., Jägers W.J. 1988, A&A 36, 347

Table 1.

| Object | $m$(%) | $\sigma$ | $m'$(%) | $\sigma$ | $A$ | $\sigma$ | Array |
|---|---|---|---|---|---|---|---|
| 0034 + 25 | 9.6 | 1.0 | 14.3 | 1.0 | -30 | 3 | C |
| E tail | 6.1 | 1.0 | 12.3 | 1.0 | -26 | 5 | |
| WS tail | 12.5 | 1.1 | 16.3 | 1.0 | -45 | 2 | |
| Inner jet | 14.9 | 1.0 | 15.1 | 1.0 | -17 | 2 | |
| 0120 + 33 | <1.1 | | 3.0 | 1.0 | - | - | C |
| E | <1.6 | - | 3.9 | 1.0 | - | - | |
| W | <1.0 | - | 2.8 | 1.0 | - | - | |
| 0149 + 35 | <1.5 | - | 5.4 | 1.5 | - | | B |
| W | <2.0 | - | 4.9 | 2.0 | -39 | - | |
| E | <2.3 | - | 8.0 | 2.3 | 40 | - | |
| core | <1.8 | - | <2.0 | - | - | - | |
| 0206 + 35 | 2.7 | 1.2 | 11.9 | 1.2 | 29 | 13 | B |
| W | 1.9 | 1.3 | 12.4 | 1.3 | -43 | 20 | |
| E | 4.6 | 1.3 | 12.0 | 1.3 | 20 | 8 | |
| core | 5.0 | 1.2 | 5.3 | 1.3 | -27 | 7 | |
| 0708 + 32 | <1.0 | - | 3.5 | 1.6 | - | - | A |
| N | <1.7 | - | 4.1 | 1.7 | - | - | |
| S | <1.5 | - | 4.1 | 1.5 | - | - | |
| core | <1.6 | - | <1.7 | | - | - | |
| 0722 + 30 | <1.3 | - | 6.9 | 1.7 | - | - | A |
| E | <1 | - | 5.7 | 1.0 | - | - | |
| W | 3.4 | 1.8 | 11.4 | 1.8 | 22 | 15 | |
| core | <1.8 | - | 2.3 | 1.8 | - | - | |
| 0755 + 37 | 5.1 | 1.0 | 12.6 | 1.0 | -54 | 6 | C |
| E | 5.7 | 1.0 | 17.2 | 1.0 | -47 | 5 | |
| W | 4.1 | 1.0 | 10.0 | 1.0 | -51 | 7 | |
| core | 1.5 | 1.0 | 1.7 | 1.0 | -35 | 19 | |
| 0800 + 24 | 5.4 | 2.0 | 8.4 | 2.0 | -25 | 16 | B |
| 0828 + 32 | 7.7 | 1.0 | 21.2 | 1.0 | -40 | 4 | C |
| E | 13.1 | 1.0 | 23.8 | 1.0 | -22 | 2 | |
| W | 6.6 | 1.0 | 19.1 | 1.0 | -61 | 4 | |
| 0836 + 29 | 5.8 | 1.2 | 10.3 | 1.2 | 22 | 6 | B |
| N | 6.8 | 1.0 | 10.3 | 1.2 | -43 | 4 | |
| S | 8.7 | 1.0 | 11.7 | 1.3 | 10 | 3 | |
| core | <1.0 | - | <1.6 | | - | - | |
| 0836 + 29*II* | 1.9 | 1.0 | 9.1 | 1.0 | 88 | 15 | C |
| N lobe | 4.5 | 1.0 | 8.9 | 1.0 | -65 | 6 | |
| S lobe | 4.6 | 1.0 | 15.7 | 1.0 | 53 | 6 | |
| core | 2.0 | 1.0 | 2.3 | 1.0 | -76 | 14 | |
| 0838 + 32 | 2.1 | 1.0 | 4.7 | 1.0 | -40 | 14 | C |
| N compact | 3.1 | 1.0 | 3.9 | 1.0 | -24 | 9 | |
| N diffuse | 8.2 | 1.0 | 10.1 | 1.0 | -80 | 4 | |

Table 1. continued

| Object | $m$(%) | $\sigma$ | $m'$(%) | $\sigma$ | $A$ | $\sigma$ | Array |
|---|---|---|---|---|---|---|---|
| 0844 + 31 | 1.8 | 1.0 | 10.4 | 1.0 | 74 | 2 | C |
| Core | 2.0 | 1.0 | 2.4 | 1.0 | -71 | 2 | |
| N jet | 11.4 | 1.0 | 11.6 | 1.0 | -75 | 4 | |
| N lobe | 2.8 | 1.0 | 12.1 | 1.0 | 43 | 2 | |
| S lobe | 2.7 | 1.0 | 6.1 | 1.0 | -85 | 2 | |
| 0908 + 37 | 2.1 | 1.4 | 6.7 | 1.4 | 4 | 9 | A+B |
| N | 4.4 | 1.0 | 8.4 | 1.0 | -2 | 7 | |
| S | <1.1 | - | 5.1 | 1.0 | - | - | |
| core | <1.3 | - | <1.3 | - | - | - | |
| 0913 + 38 | 5.9 | 1.1 | 10.8 | 1.1 | 4 | 5 | B |
| W | 6.4 | 1.3 | 11.5 | 1.3 | 30 | 6 | |
| E | 5.9 | 1.4 | 10.1 | 1.4 | -45 | 7 | |
| 0915 + 32 | 4.8 | 1.0 | 12.8 | 1.0 | -6 | 6 | C |
| N jet | 2.6 | 1.0 | 8.6 | 1.0 | 68 | 11 | |
| S lobe | 19.2 | 1.0 | 21.4 | 1.0 | 2 | 2 | |
| core | 6.0 | 1.0 | 12.7 | 1.0 | -41 | 5 | |
| 0922 + 36 | <2.0 | - | 2.3 | 1.0 | - | - | C |
| N lobe | <2.0 | - | 1.6 | 1.0 | - | - | |
| S lobe | 2.9 | 1.0 | 3.6 | 1.0 | 8 | 10 | |
| S compact | 2.9 | 1.0 | 3.6 | 1.0 | 8 | 10 | |
| core | <6.0 | - | 2.6 | 1.0 | - | - | |
| 1003 + 26 | <1 | - | <1.4 | - | - | - | A |
| 1005 + 28 | 4.0 | 1.0 | 10.3 | 1.0 | 58 | 7 | C |
| N lobe | 2.3 | 1.0 | 9.3 | 1.0 | 52 | 12 | |
| S lobe | 2.2 | 1.0 | 12.6 | 1.0 | 50 | 13 | |
| core | 9.0 | 1.1 | 9.8 | 1.1 | 63 | 4 | |
| 1040 + 30 | 2.2 | 1.1 | 3.4 | 1.1 | 39 | 14 | B |
| 1102 + 30 | 8.3 | 1.0 | 12.3 | 1.0 | -83 | 3 | C |
| E lobe | 12.7 | 1.0 | 15.2 | 1.0 | -85 | 2 | |
| W lobe | 3.8 | 1.0 | 9.8 | 1.0 | -75 | 7 | |
| core | <3.1 | - | 2.7 | 1.1 | - | - | |
| 1108 + 27 | 10.9 | 1.4 | 13.8 | 1.4 | -30 | 4 | B+C |
| E | 16.2 | 5.4 | 27.1 | 5.4 | 21 | 10 | |
| W | 13.5 | 1.4 | 15.6 | 1.4 | -28 | 3 | |
| core | <1.9 | - | 2.5 | 1.6 | - | - | |
| 1113 + 29 | 3.7 | 1.2 | 14.0 | 1.2 | -92 | 9 | B |
| W | 8.5 | 1.2 | 15.6 | 1.2 | -4 | 4 | |
| E | 2.1 | 1.3 | 12.2 | 1.3 | -25 | 18 | |
| core | 5.8 | 1.6 | 6.4 | 1.6 | 43 | 8 | |

Table 1. continued

| Object | $m$(%) | $\sigma$ | $m'$(%) | $\sigma$ | $A$ | $\sigma$ | Array |
|---|---|---|---|---|---|---|---|
| 1116 + 28 | 1.6 | 1.0 | 7.6 | 1.0 | -74 | 18 | C |
| E tail | 6.0 | 1.0 | 12.0 | 1.0 | 56 | 6 | |
| W tail | 3.2 | 1.0 | 6.8 | 1.0 | -29 | 9 | |
| core | 4.7 | 1.0 | 5.1 | 1.0 | -67 | 6 | |
| 1122 + 39 | 10.1 | 1.3 | 12.1 | 1.3 | 27 | 4 | B+C |
| W | 10.5 | 1.5 | 12.2 | 1.5 | 30 | 4 | |
| E | 10.6 | 1.5 | 12.9 | 1.5 | 26 | 4 | |
| core | <1.6 | - | 1.7 | 1.4 | - | - | |
| 1141 + 37 | 2.4 | 1.0 | 6.0 | 1.0 | -79 | 12 | C |
| N lobe | 2.7 | 1.0 | 5.7 | 1.0 | -76 | 11 | |
| S lobe | 4.1 | 1.0 | 6.4 | 1.0 | -60 | 7 | |
| 1204 + 24 | 5.6 | 2.0 | 15.3 | 2.0 | -42 | 10 | A |
| N | 9.4 | 2.1 | 16.8 | 2.1 | -36 | 6 | |
| S | 7.8 | 1.8 | 19.3 | 1.8 | 37 | 7 | |
| core | <2.0 | - | <2.0 | - | - | - | |
| 1204 + 34 | 4.0 | 1.2 | 12.3 | 1.2 | 33 | 9 | B |
| N | 3.4 | 1.2 | 13.5 | 1.2 | 2 | 10 | |
| S | 5.6 | 1.2 | 12.3 | 1.2 | 25 | 6 | |
| core | <1.1 | - | <1.5 | - | - | - | |
| 1243 + 26 | 3.1 | 1.0 | 7.1 | 1.0 | 67 | 9 | C |
| N lobe | 12.0 | 1.0 | 14.0 | 1.0 | 89 | 2 | |
| S lobe | <1.9 | - | 5.1 | 1.0 | - | - | |
| core | 5.3 | 1.0 | 7.3 | 1.0 | 60 | 5 | |
| 1254 + 27 | 3.1 | 1.7 | 7.0 | 1.7 | 36 | 16 | B |
| N | 4.7 | 1.9 | 9.5 | 1.9 | 40 | 12 | |
| S | <1.1 | - | 3.7 | 1.1 | - | - | |
| 1300 + 32 | < 1.0 | - | 1.6 | 1.0 | - | - | C |
| NE lobe | < 1.0 | - | 1.6 | 1.0 | - | - | |
| NW lobe | < 3.8 | - | 3.4 | 1.3 | - | - | |
| S lobe | <1.6 | - | 1.5 | 1.0 | - | - | |
| 1303 + 31 | 2.6 | 2.3 | 4.7 | 2.3 | -20 | 25 | A |
| 1316 + 29 | 12.8 | 1.0 | 15.7 | 1.0 | -76 | 2 | C |
| E lobe | 14.8 | 1.0 | 17.5 | 1.0 | -73 | 2 | |
| W lobe | 10.3 | 1.0 | 13.5 | 1.0 | -79 | 3 | |
| core | 15.3 | 1.0 | 15.7 | 1.0 | -86 | 2 | |
| 1317 + 33 | <2.0 | - | 10.5 | 2.0 | - | - | A |
| N | <1.9 | - | 9.8 | 1.9 | - | - | |
| S | <2.7 | - | 15.1 | 2.7 | - | - | |
| core | <2.6 | - | 3.4 | 2.6 | - | - | |
| 1322 + 36 | 4.6 | 1.1 | 13.6 | 1.1 | 11 | 7 | B |
| N | 8.0 | 1.2 | 12.4 | 1.2 | 8 | 4 | |
| S | 8.3 | 1.2 | 18.3 | 1.2 | 8 | 4 | |
| core | 1.8 | 1.2 | 2.6 | 1.2 | 25 | 19 | |

**Table 1.** continued

| Object | $m$(%) | $\sigma$ | $m'$(%) | $\sigma$ | $A$ | $\sigma$ | Array |
|---|---|---|---|---|---|---|---|
| 1339 + 26 | <1.5 | - | <1.8 | - | - | - | C |
| head | <1.6 | - | <1.6 | - | - | - | |
| 1347 + 28 | 6.5 | 1.3 | 8.2 | 1.3 | 42 | 6 | B |
| N | 6.8 | 1.4 | 7.9 | 1.4 | 45 | 6 | |
| S | 5.4 | 1.5 | 7.3 | 1.5 | 41 | 8 | |
| core | 4.9 | 2.6 | 4.9 | 2.6 | 36 | 15 | |
| 1357 + 28 | 2.9 | 1.0 | 5.0 | 1.0 | 79 | 10 | C |
| N lobe | 2.5 | 1.0 | 5.8 | 1.0 | 81 | 11 | |
| S lobe | 2.1 | 1.0 | 3.9 | 1.0 | 65 | 14 | |
| core | 4.8 | 1.0 | 5.3 | 1.0 | -6 | 6 | |
| 1358 + 30 | 2.6 | 1.1 | 8.7 | 1.1 | -8 | 11 | C |
| lobe N | 3.5 | 1.2 | 9.5 | 1.2 | 1.4 | 8 | |
| lobe S | 4.2 | 1.3 | 5.9 | 1.3 | 35 | 7 | |
| 1422 + 26 | 6.2 | 1.0 | 8.0 | 1.0 | -64 | 5 | C |
| E lobe | 4.6 | 1.0 | 5.8 | 1.0 | -77 | 6 | |
| W lobe | 8.7 | 1.0 | 10.3 | 1.0 | -57 | 3 | |
| 1430 + 25 | 1.7 | 1.1 | 10.8 | 1.1 | -30 | 19 | B |
| 1441 + 26 | 6.8 | 1.0 | 9.3 | 1.0 | 11 | 4 | C |
| E lobe | 10.7 | 1.0 | 11.6 | 1.0 | 19 | 3 | |
| W lobe | 1.9 | 1.0 | 3.6 | 1.0 | -28 | 15 | |
| 1450 + 28 | <1.5 | - | 7.8 | 1.7 | - | - | B |
| W | <2.9 | - | 8.2 | 2.2 | - | - | |
| E | <1.8 | - | 7.5 | 1.8 | - | - | |
| 1455 + 28 | 2.4 | 1.0 | 7.9 | 1.0 | -15 | 12 | C |
| N lobe | 1.3 | 1.0 | 7.8 | 1.0 | -22 | 22 | |
| S lobe | 3.9 | 1.0 | 7.8 | 1.0 | -14 | 7 | |
| 1457 + 29 | 11.9 | 1.0 | 12.6 | 1.0 | 21 | 2 | C |
| N lobe | 13.9 | 1.0 | 14.5 | 1.0 | 21 | 2 | |
| S lobe | 9.7 | 1.0 | 10.6 | 1.0 | 21 | 3 | |
| 1512 + 30 | 11.8 | 1.1 | 12.7 | 1.1 | 17 | 2 | C |
| N lobe | 8.0 | 1.5 | 8.2 | 1.5 | 32 | 4 | |
| S lobe | 17.1 | 1.4 | 17,1 | 1.4 | 10 | 2 | |
| 1521 + 28 | 3.9 | 1.0 | 10.7 | 1.0 | -18 | 7 | C |
| N lobe | 3.6 | 1.0 | 3.6 | 1.0 | 64 | 8 | |
| S lobe | 9.1 | 1.0 | 15.5 | 1.0 | -22 | 3 | |
| core | 5.7 | 1.0 | 5.7 | 1.0 | 46 | 5 | |
| 1525 + 29 | <1.8 | - | 12.8 | 1.8 | - | - | A |
| N lobe | 1.8 | 1.4 | 12.9 | 1.4 | 13 | 22 | |
| S | <1.4 | - | 12.8 | 1.3 | - | - | |

Table 1. continued

| Object | $m$(%) | $\sigma$ | $m'$(%) | $\sigma$ | $A$ | $\sigma$ | Array |
|---|---|---|---|---|---|---|---|
| 1527 + 30 | <1.6 | - | 5.9 | 1.6 | 39 | - | B |
| E lobe | <2.0 | - | 7.2 | 2.0 | -44 | - | |
| W lobe | <2.0 | - | 7.4 | 2.0 | 18 | - | |
| core | 2.6 | 1.6 | 2.6 | 1.6 | -43 | 18 | |
| 1528 + 29 | 4.3 | 1.0 | 8.6 | 1.0 | -87 | 7 | C |
| E lobe | 6.6 | 1.0 | 8.6 | 1.0 | 74 | 4 | |
| W lobe | 5.8 | 1.0 | 8.5 | 1.0 | -64 | 5 | |
| core | 6.4 | 1.2 | 7.3 | 1.2 | 49 | 5 | |
| 1553 + 24 | 3.4 | 1.1 | 7.1 | 1.1 | 6 | 9 | C |
| W | 3.5 | 1.4 | 9.2 | 1.4 | -8 | 12 | |
| E | 5.4 | 1.5 | 6.2 | 1.5 | -37 | 8 | |
| 1609 + 31 | 11.6 | 1.3 | 14.6 | 1.3 | 16 | 3 | B |
| N | 13.3 | 1.4 | 15.1 | 1.4 | 26 | 3 | |
| S | 11.9 | 1.6 | 14.0 | 1.6 | 3 | 4 | |
| 1613 + 27 | 3.5 | 1.9 | 10.0 | 1.9 | 25 | 16 | B |
| E | 2.9 | 1.2 | 10.6 | 1.2 | 27 | 12 | |
| W | 4.1 | 1.2 | 9.5 | 1.2 | 24 | 8 | |
| 1615 + 32 | 4.1 | 1.0 | 4.6 | 1.0 | -59 | 7 | C |
| N lobe | 4.6 | 1.0 | 5.0 | 1.0 | -58 | 6 | |
| S lobe | 3.6 | 1.0 | 4.1 | 1.0 | -61 | 8 | |
| 1621 + 38 | <1.3 | - | 3.1 | 1.3 | - | - | A |
| N | <1.0 | - | <1.8 | - | - | - | |
| S | 2.3 | 1.2 | 3.1 | 1.2 | -12 | 15 | |
| Tail | 2.2 | 1.5 | 5.1 | 1.5 | 12 | 20 | |
| 1626 + 39 | 3.2 | 1.1 | 3.4 | 1.1 | -15 | 10 | B |
| W | 3.6 | 1.1 | 3.7 | 1.1 | -18 | 9 | |
| E | 2.3 | 1.1 | 3.1 | 1.1 | 16 | 14 | |
| core | 2.7 | 1.3 | 2.9 | 1.3 | -15 | 14 | |
| 1638 + 32 | 3.4 | 1.1 | 7.0 | 1.1 | -25 | 9 | B+C |
| E | 2.8 | 1.9 | 6.5 | 1.9 | -36 | 19 | |
| W | 6.2 | 1.2 | 12.3 | 1.2 | -27 | 6 | |
| Central | <1.1 | - | 1.6 | 1.1 | - | - | |
| 1643 + 27 | 2.9 | 1.0 | 5.3 | 1.0 | 85 | 10 | C |
| N lobe | 6.2 | 1.0 | 7.0 | 1.0 | 89 | 5 | |
| S lobe | <1.2 | - | 3.9 | 1.0 | - | - | |
| core | <4.6 | - | 2.4 | 1.0 | - | - | |
| 1657 + 32 | 1.5 | 1.0 | 4.9 | 1.0 | 19 | 19 | C |

**Table 1.** continued

| Object | $m$(%) | $\sigma$ | $m'$(%) | $\sigma$ | $A$ | $\sigma$ | Array |
|---|---|---|---|---|---|---|---|
| 1658 + 30 | 7.4 | 1.0 | 13.1 | 1.0 | -76 | 4 | C |
| E lobe | 8.0 | 1.0 | 13.3 | 1.0 | -49 | 4 | |
| W lobe | 10.2 | 1.0 | 15.4 | 1.0 | -86 | 3 | |
| core | 3.8 | 1.0 | 4.3 | 1.0 | -77 | 8 | |
| 1658 + 32 | 2.3 | 1.0 | 2.9 | 1.0 | -49 | 12 | C |
| 1726 + 31 | 1.8 | 1.0 | 6.0 | 1.0 | 86 | 2 | C |
| E lobe | 3.3 | 1.0 | 6.1 | 1.0 | -86 | 9 | |
| W lobe | <1.9 | - | 5.9 | 1.0 | - | - | |
| 1747 + 30 | 4.7 | 2.0 | 19.1 | 2.0 | 29 | 12 | B+C |
| N | 5.1 | 2.0 | 12.2 | 2.0 | 7 | 11 | |
| S | 5.8 | 2.0 | 20.0 | 2.0 | 33 | 10 | |
| core | <2.0 | - | <2.4 | - | - | - | |
| 1752 + 32 | 10.8 | 1.4 | 13.6 | 1.4 | -4 | 4 | C |
| W | 7.0 | 1.9 | 13.4 | 1.9 | -3 | 8 | |
| E | 16.3 | 1.8 | 18.3 | 1.8 | -7 | 3 | |
| core | 8.1 | 1.3 | 8.3 | 1.3 | 2 | 5 | |
| 1827 + 32 | <1.9 | - | 6.2 | 1.0 | - | - | C |
| N lobe | 6.8 | 1.0 | 11.9 | 1.0 | -14 | 4 | |
| S lobe | 1.5 | 1.0 | 6.2 | 1.0 | 90 | 19 | |
| core | <1.8 | - | 1.4 | 1.0 | - | - | |
| 1833 + 32 | 3.7 | 1.1 | 13.1 | 1.1 | 21 | 9 | B |
| S lobe | 8.2 | 1.1 | 14.8 | 1.1 | 11 | 4 | |
| N lobe | 2.5 | 1.1 | 13.2 | 1.1 | -43 | 13 | |
| N h.s. | 10.7 | 1.1 | 12.9 | 1.1 | 6 | 3 | |
| core | 3.5 | 1.1 | 3.6 | 1.1 | -3 | 9 | |
| 1855 + 37 | <1 | - | <1.0 | - | - | - | A |
| 2116 + 26 | 5.1 | 1.4 | 9.1 | 1.4 | 41 | 8 | B+C |
| N | 3.0 | 2.0 | 12.2 | 2.0 | 36 | 19 | |
| S | 11.4 | 1.8 | 17.2 | 1.8 | 34 | 5 | |
| core | <1.0 | - | <1.2 | - | - | - | |
| 2236 + 35 | 13.6 | 1.3 | 20.5 | 1.3 | 39 | 3 | B |
| E | 19.5 | 1.4 | 19.1 | 1.4 | 42 | 2 | |
| W | 9.1 | 1.4 | 23.4 | 1.4 | 33 | 4 | |
| core | 5.9 | 2.0 | 6.2 | 2.0 | 36 | 10 | |

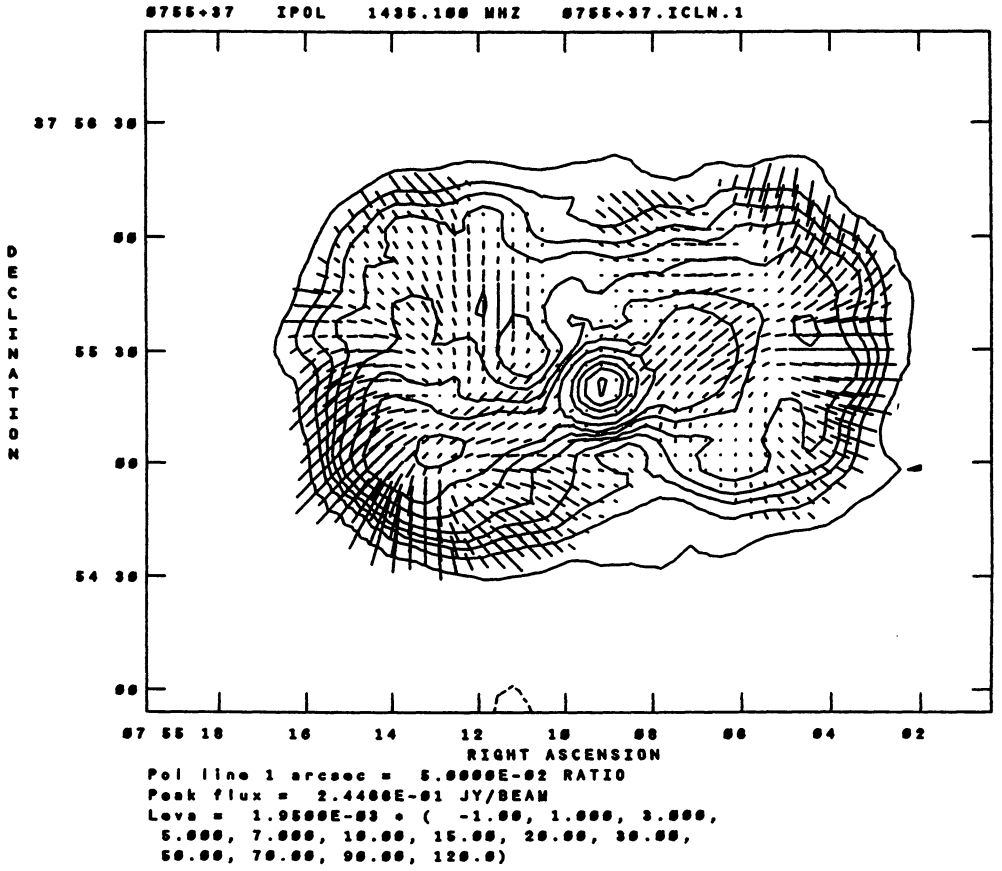


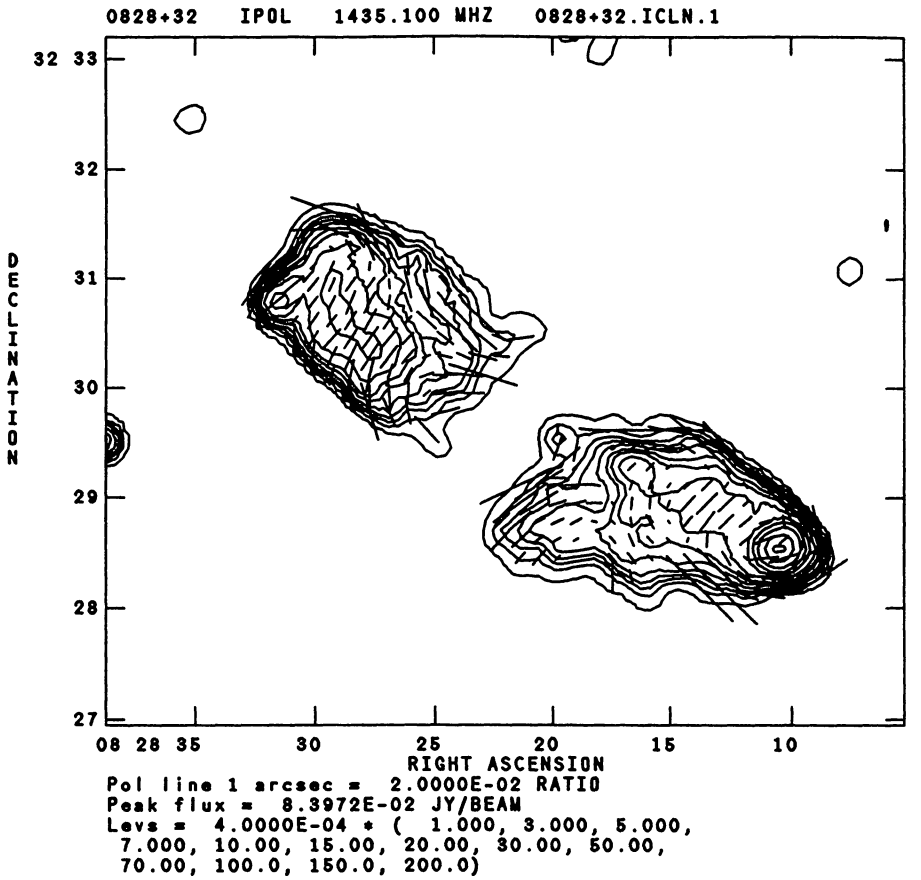


Fig. 1. Contour plots of total intensity with superposed vectors representing the fractional polarization and position angle

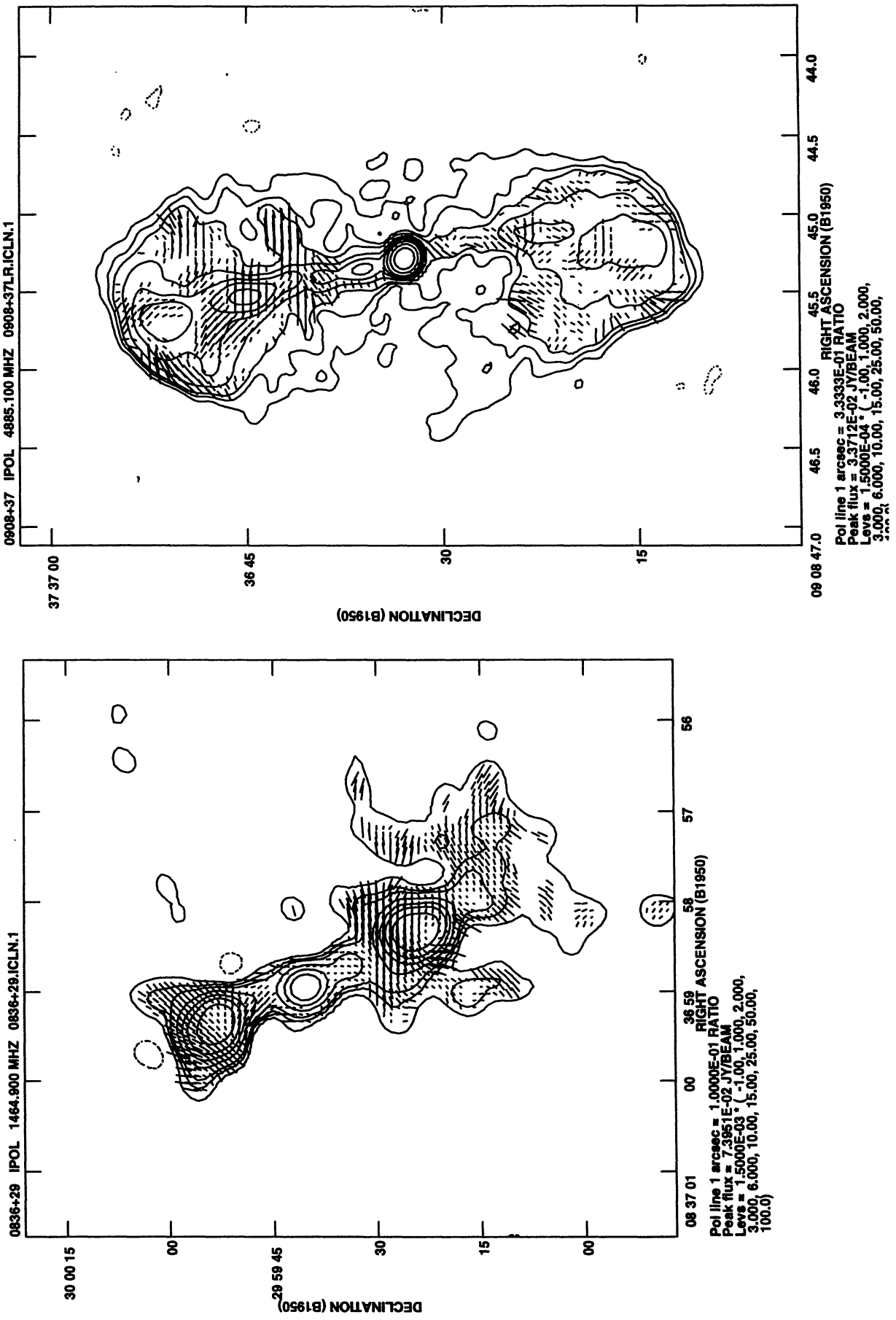


Fig. 1. continued

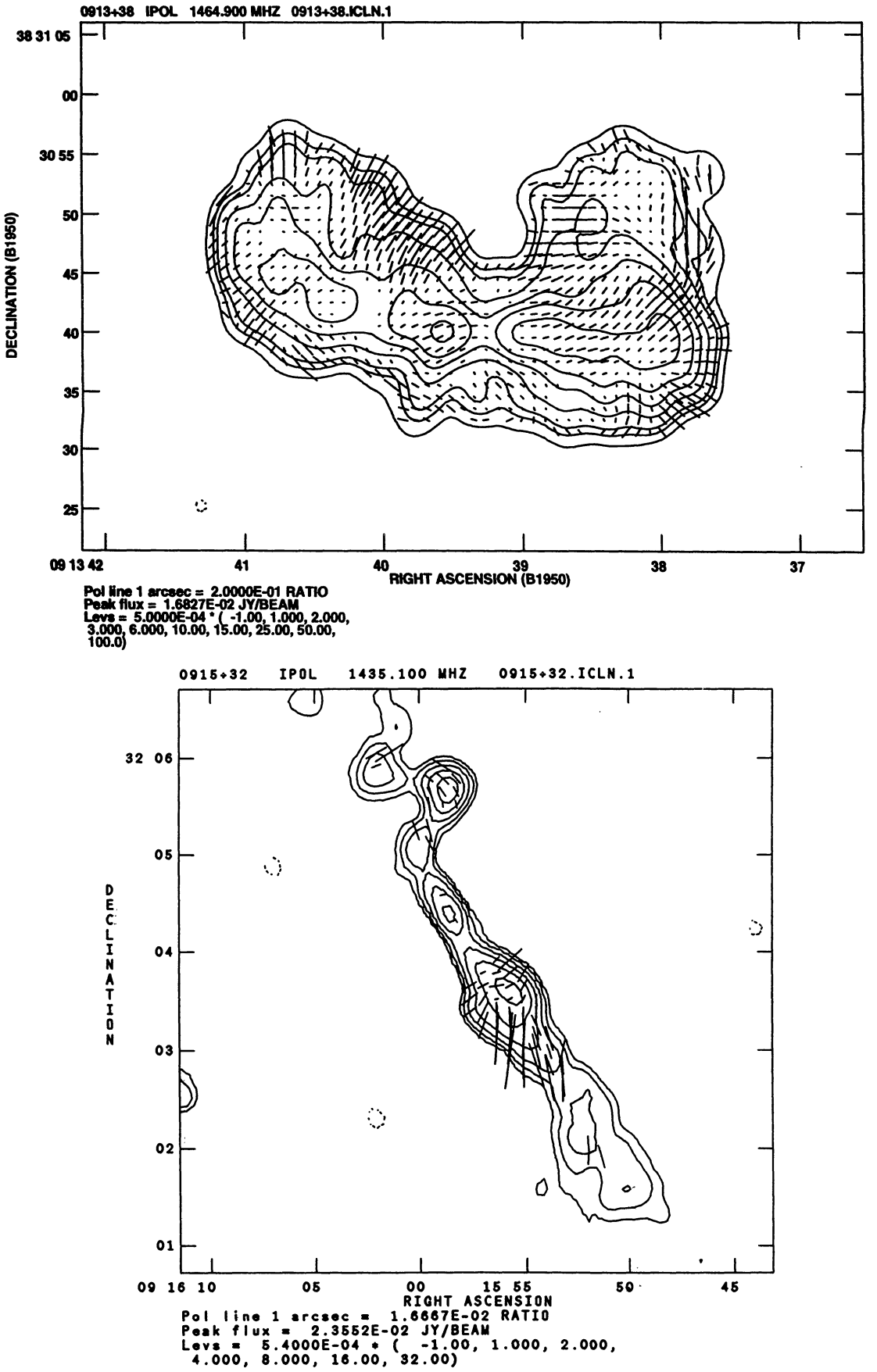


Fig. 1. continued

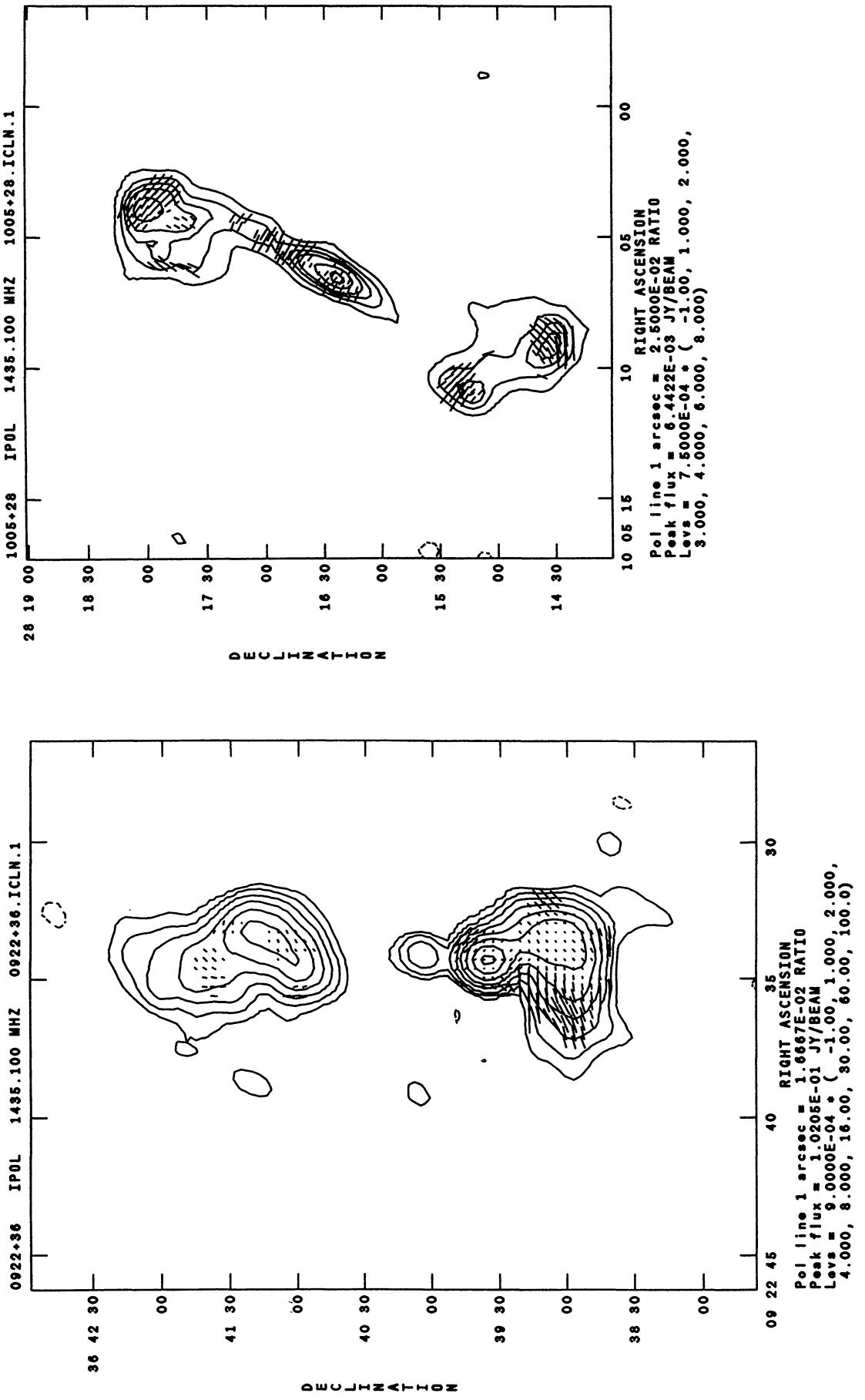


Fig. 1. continued

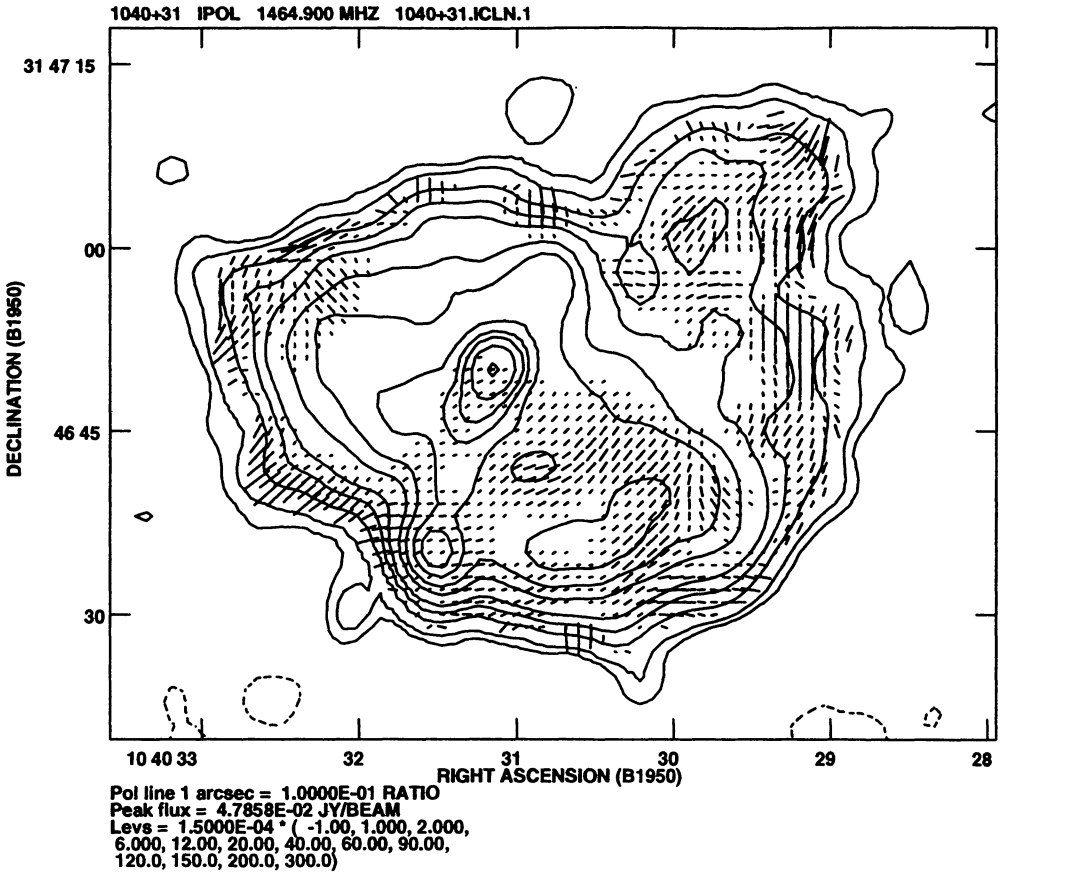


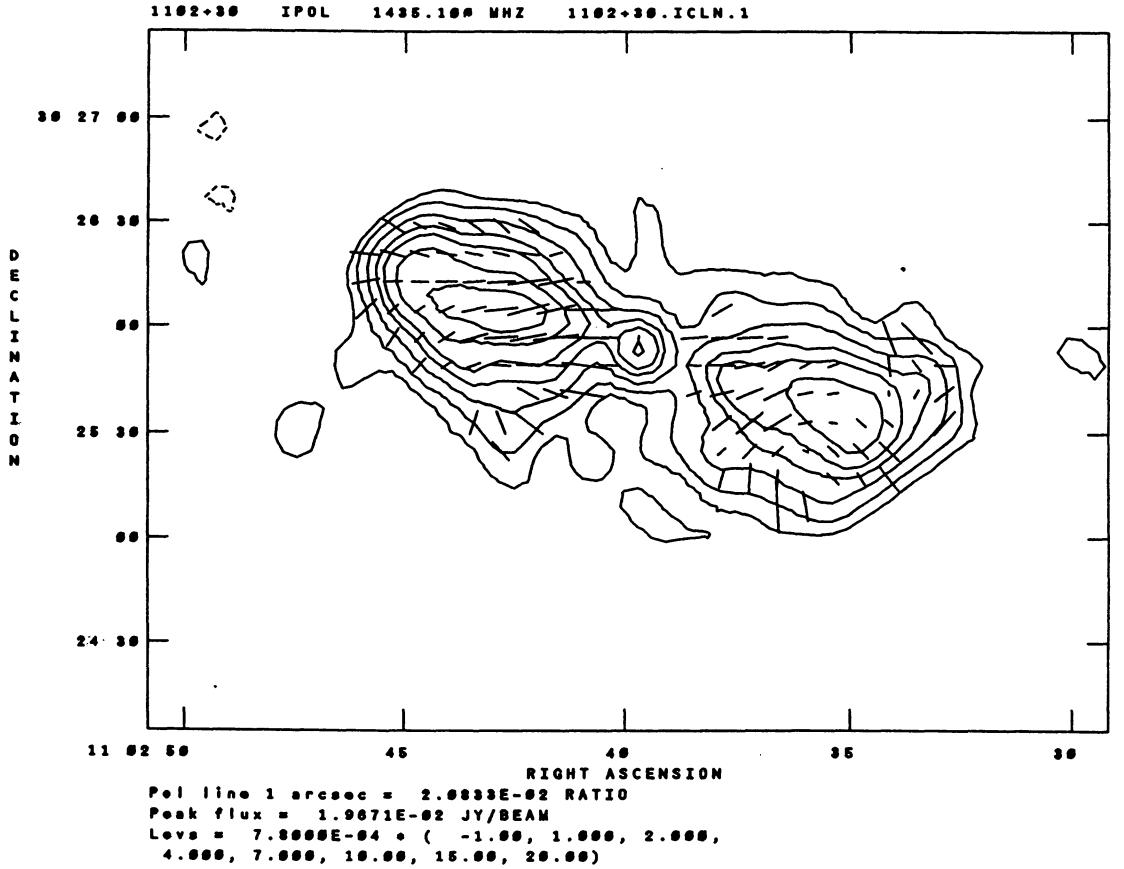


**Fig. 1.** continued

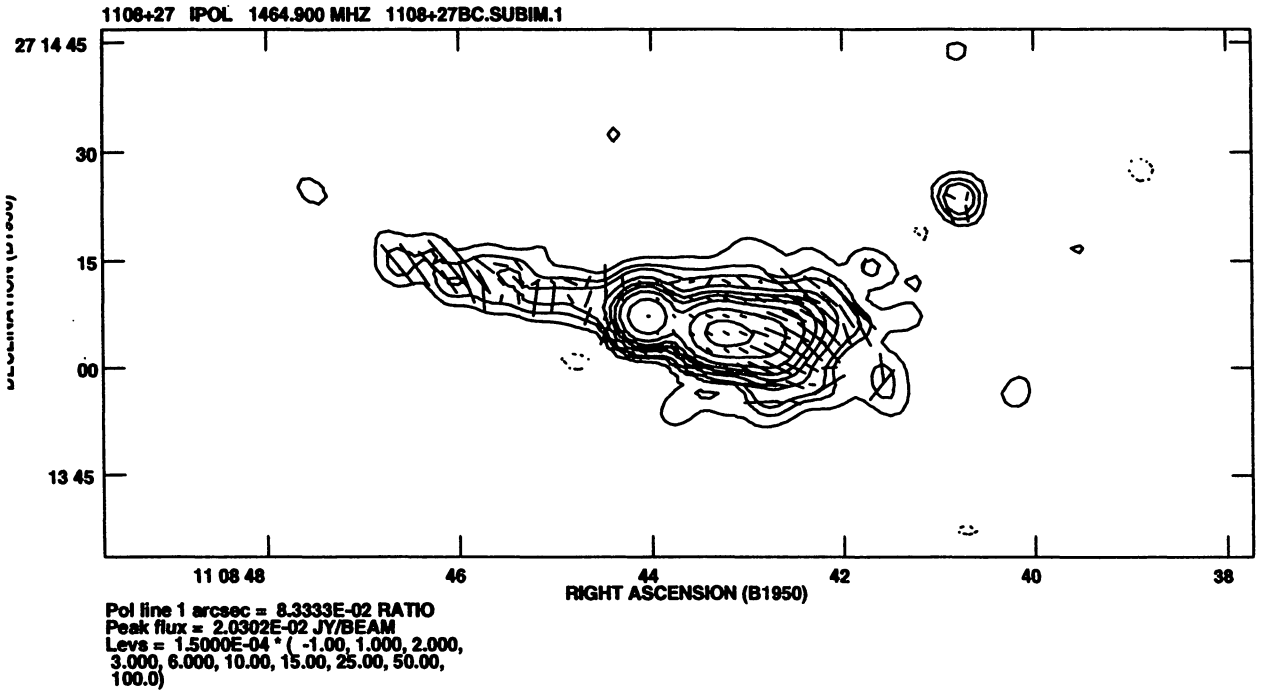


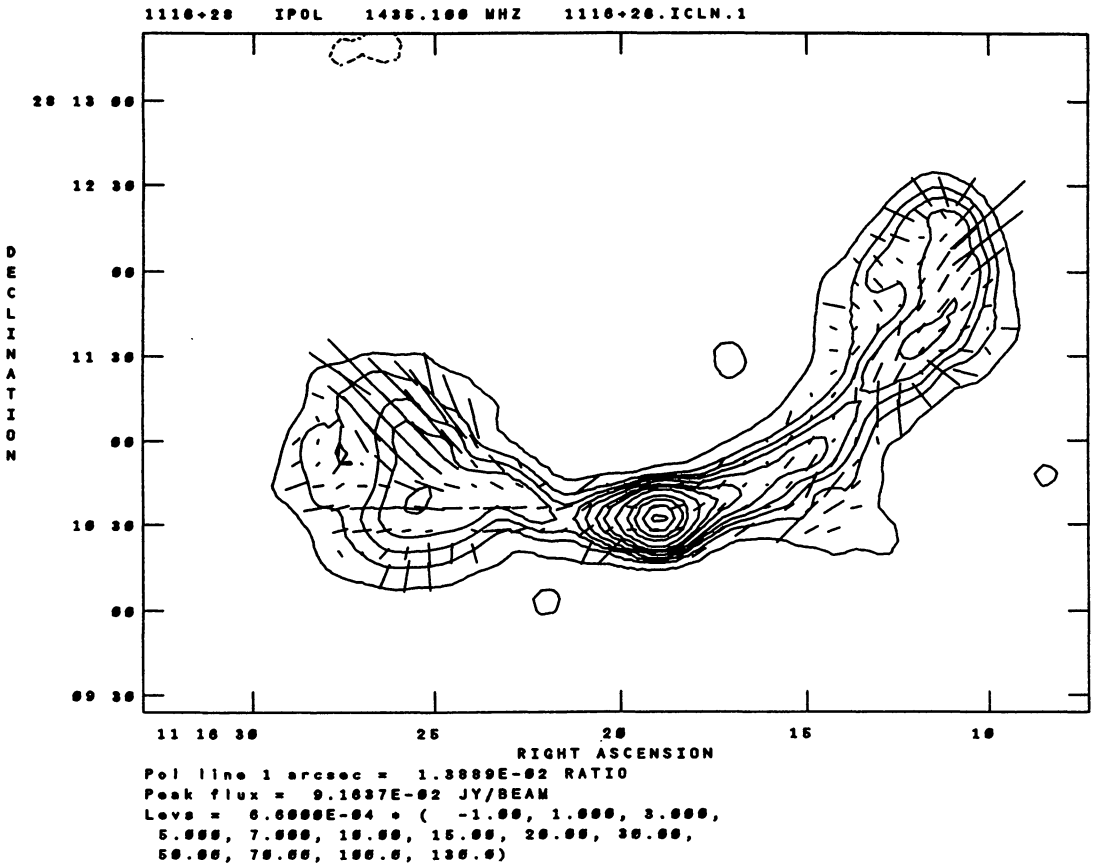


Fig. 1. continued

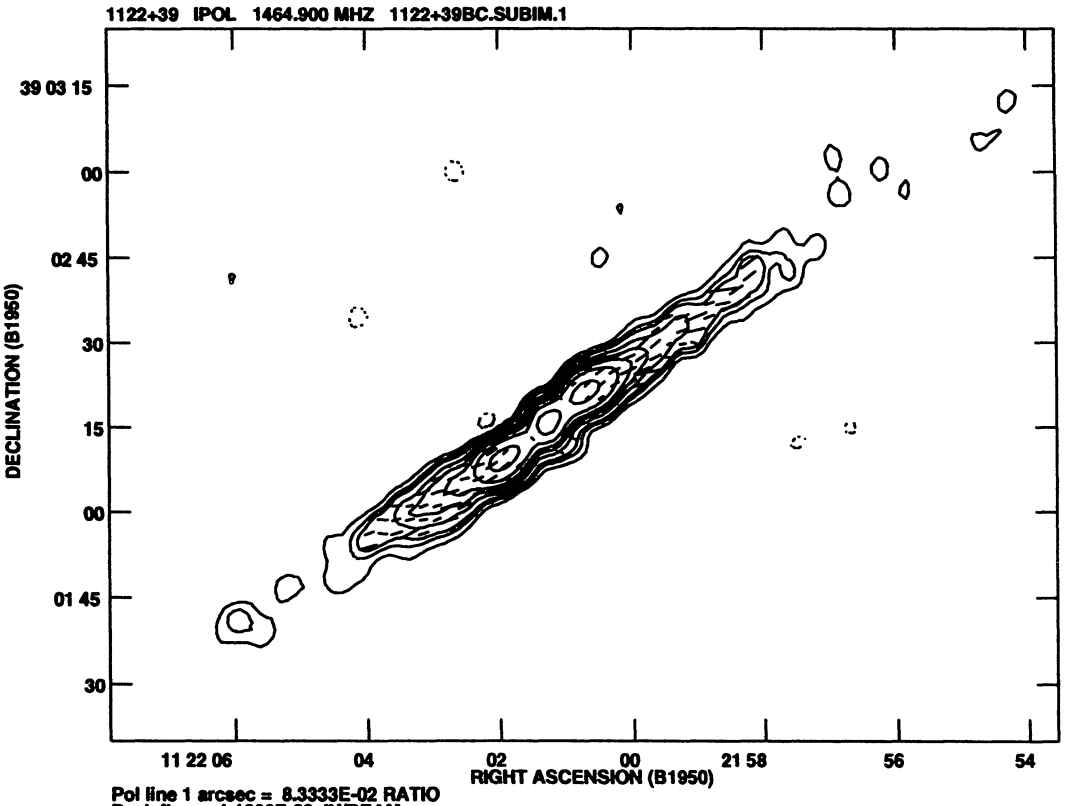


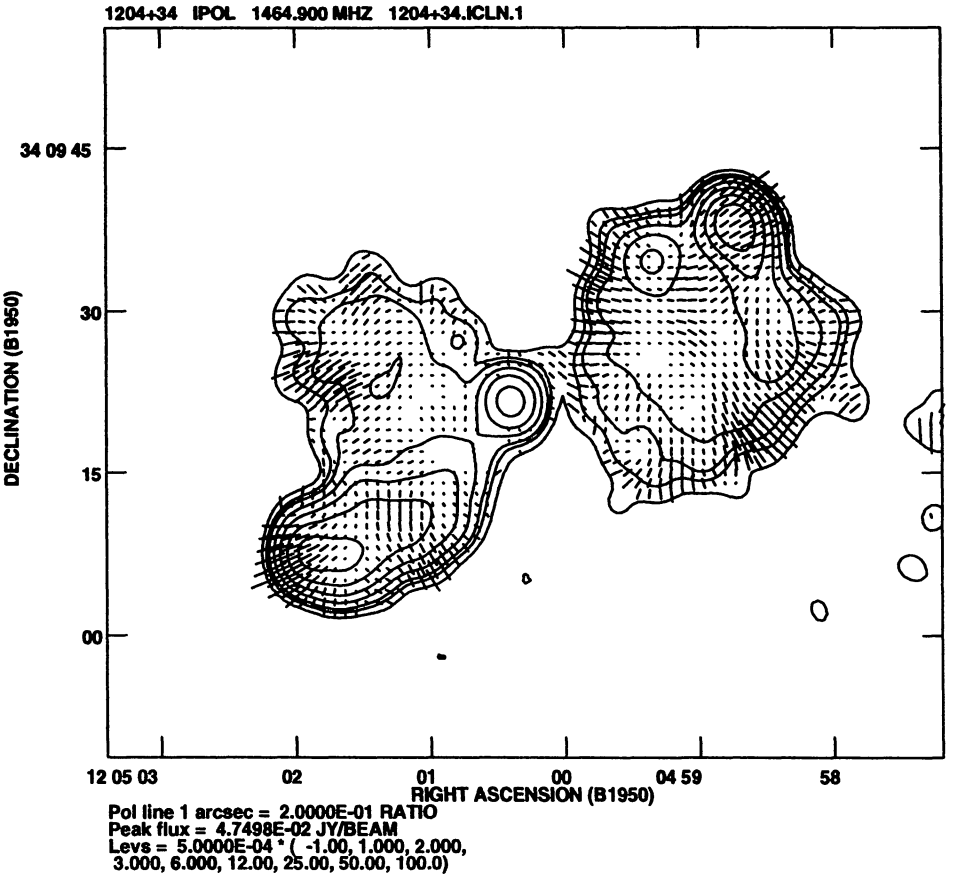


Fig. 1. continued

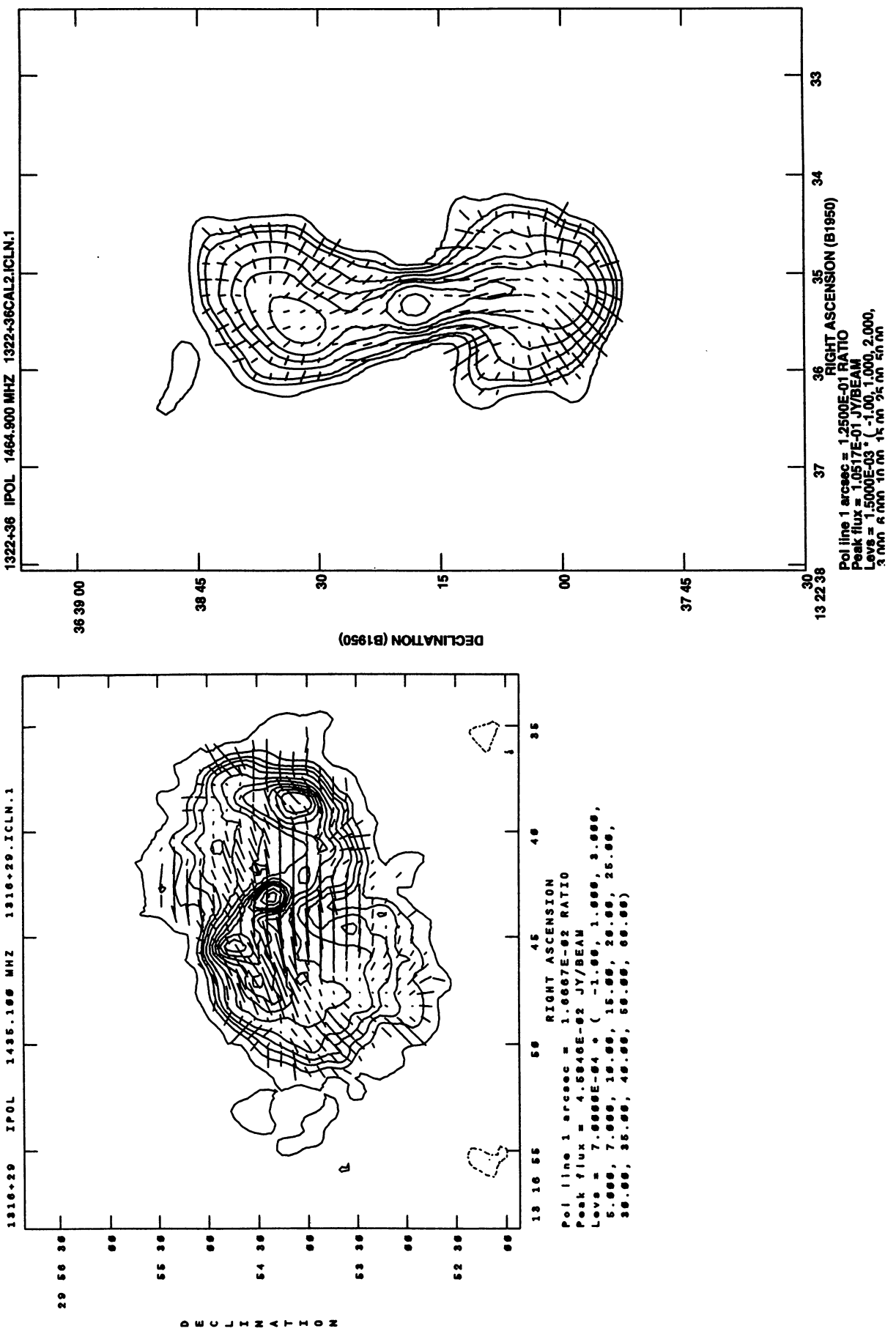


Fig. 1. continued

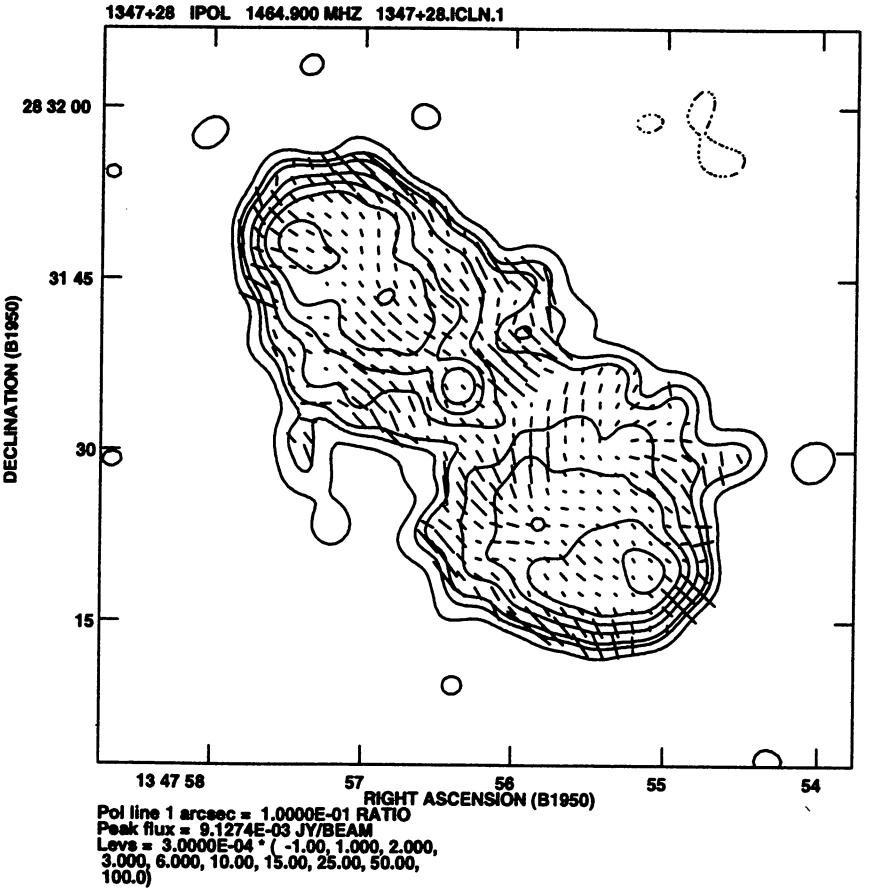


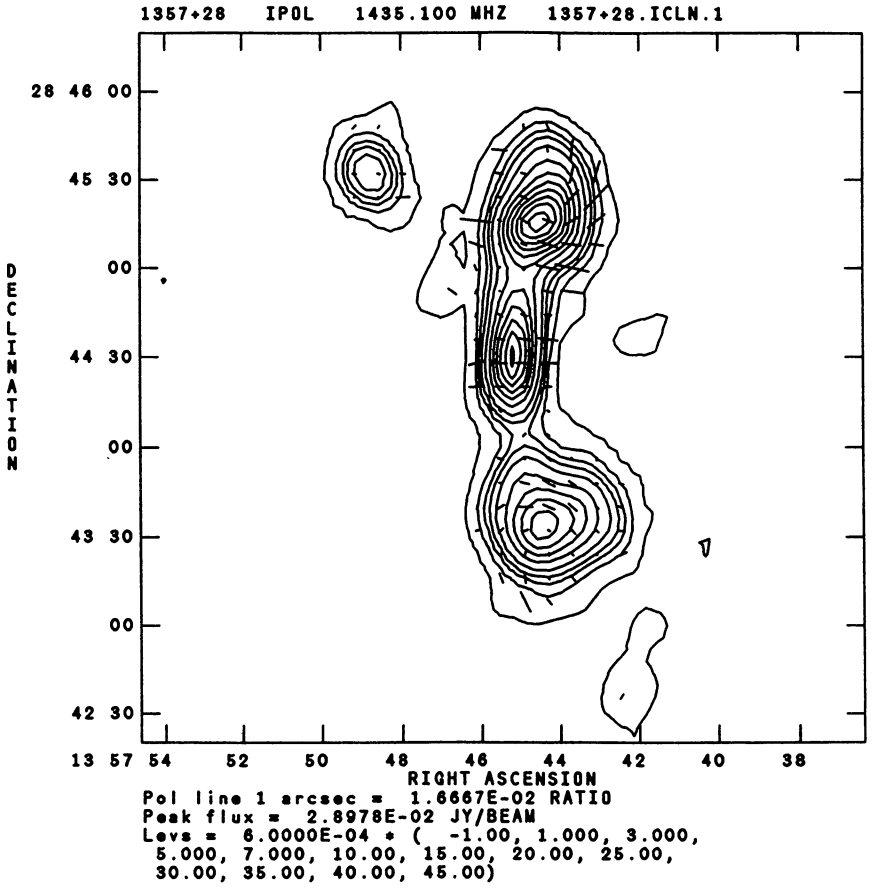


Fig. 1. continued

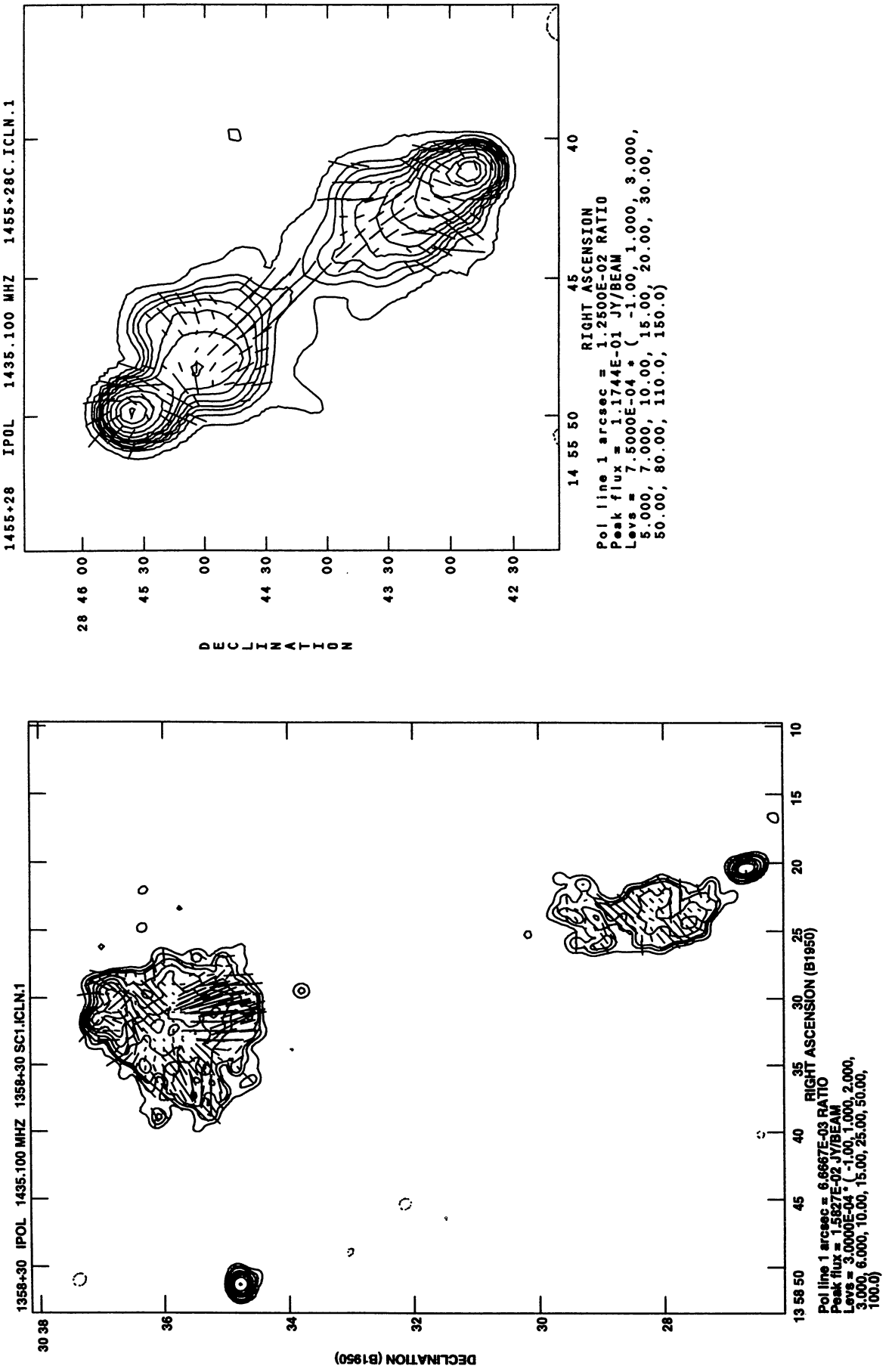


Fig. 1. continued

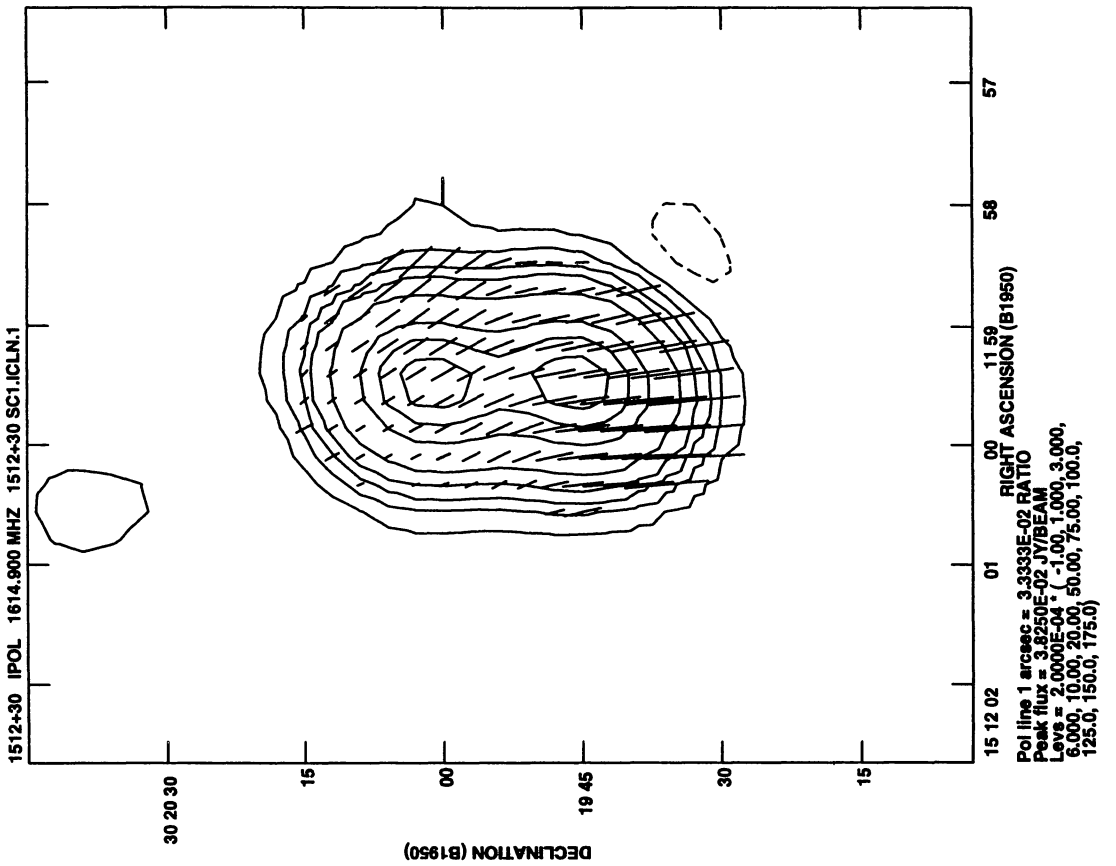


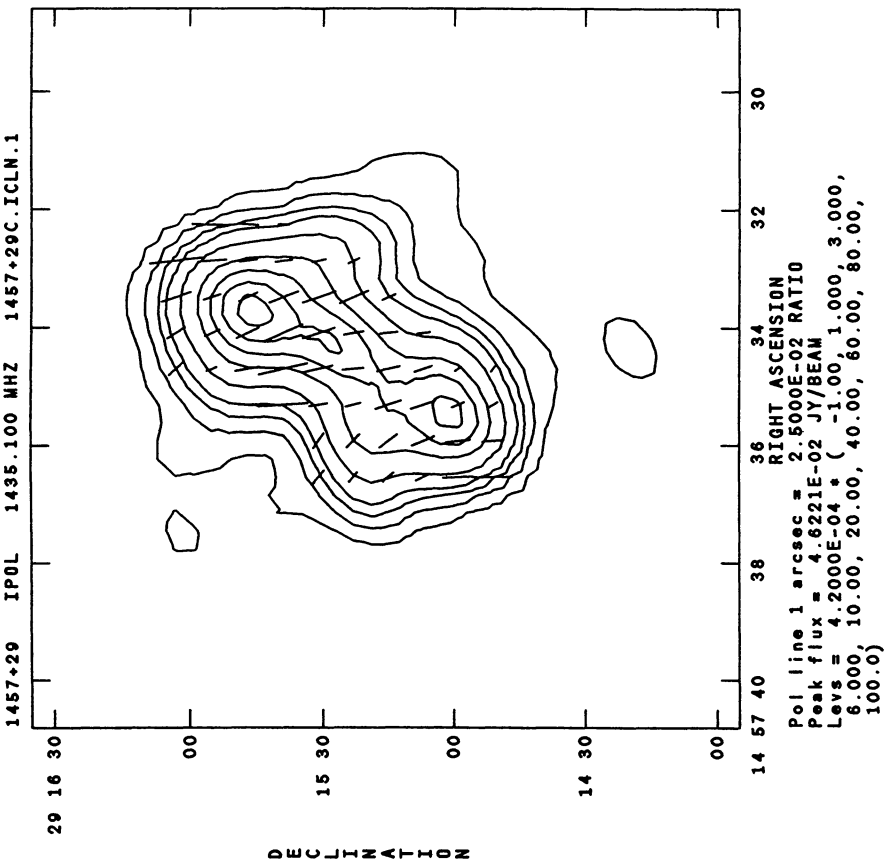


Fig. 1. continued

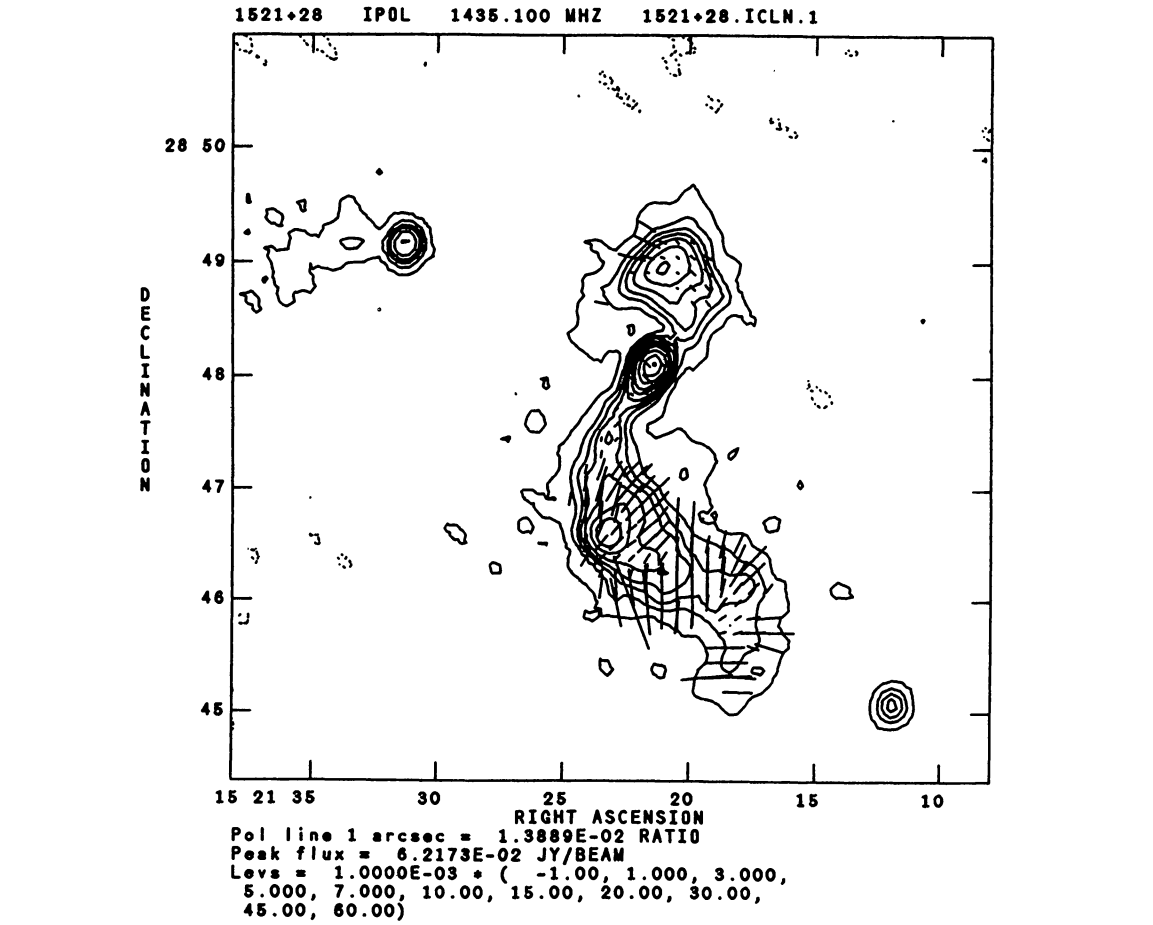


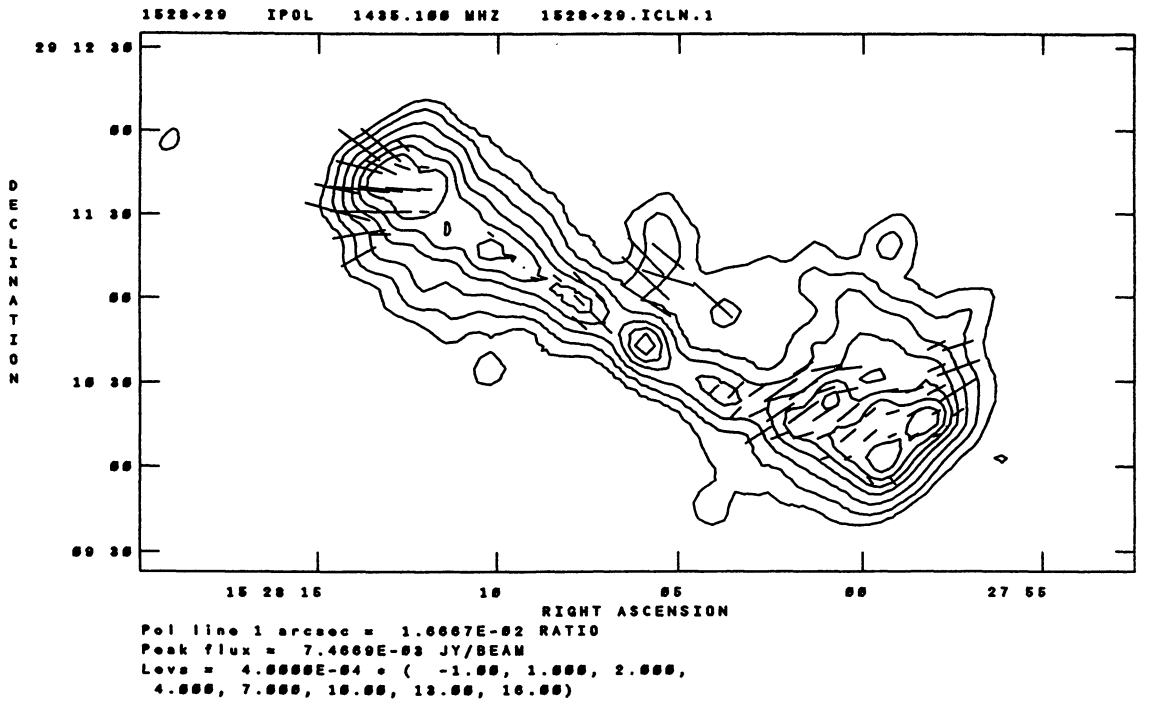


Fig. 1. continued

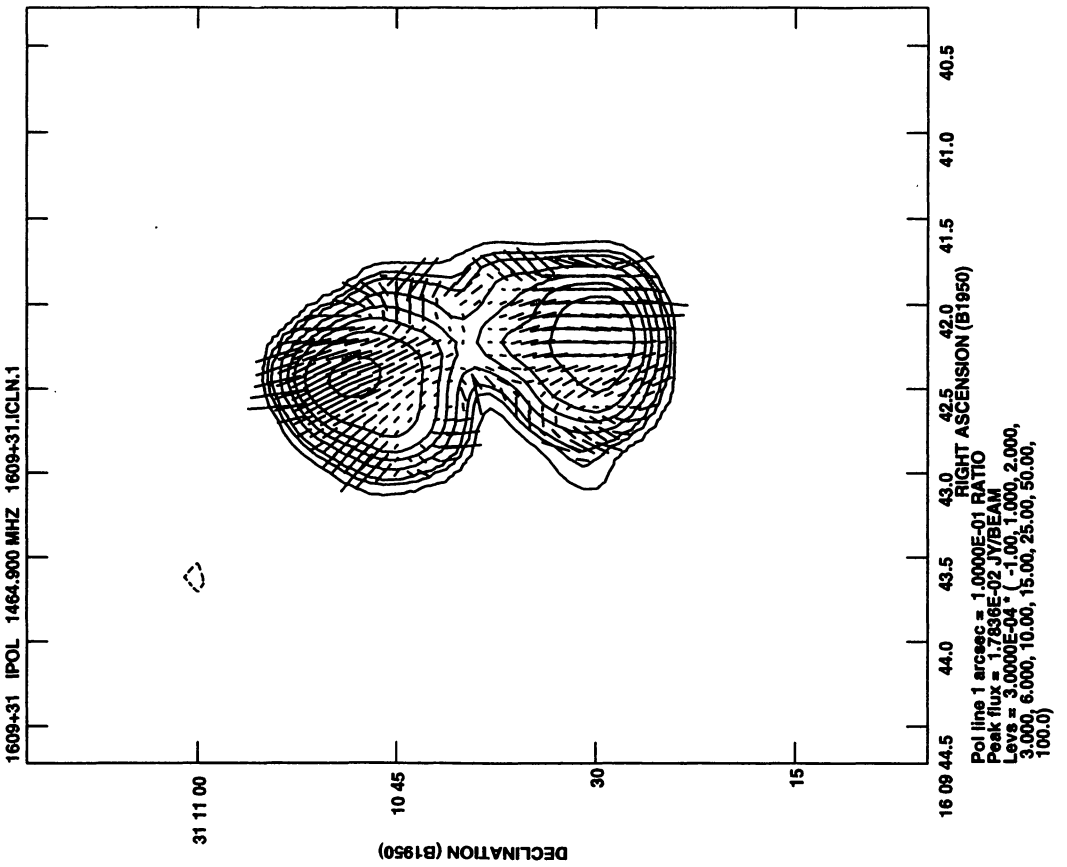


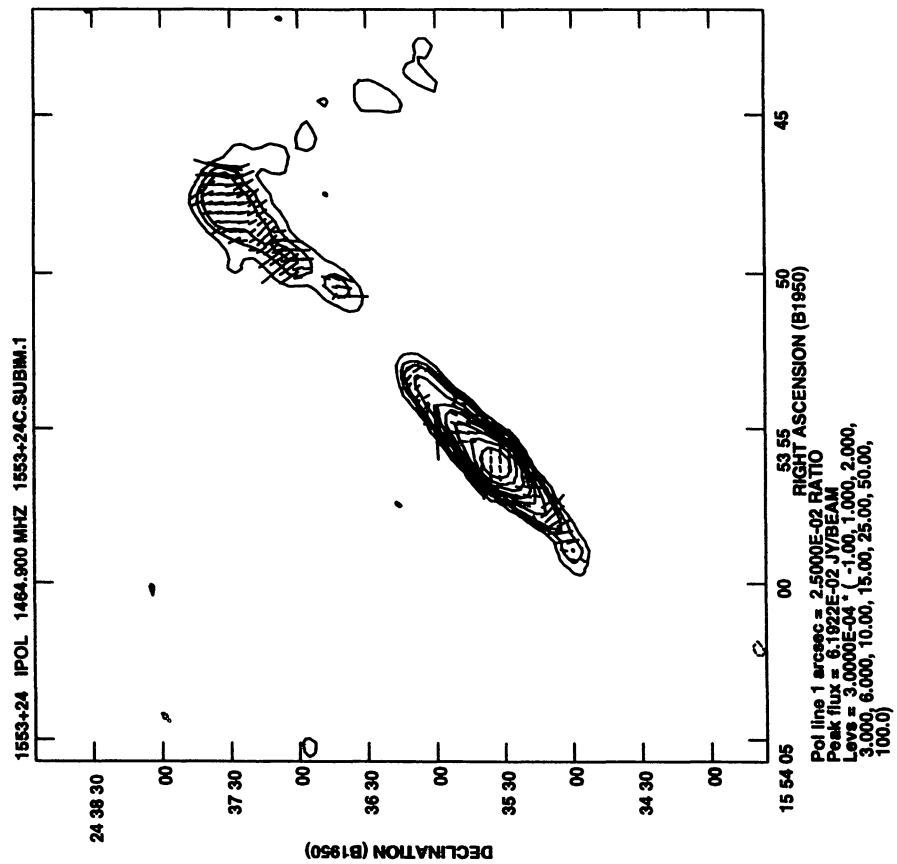


Fig. 1. continued

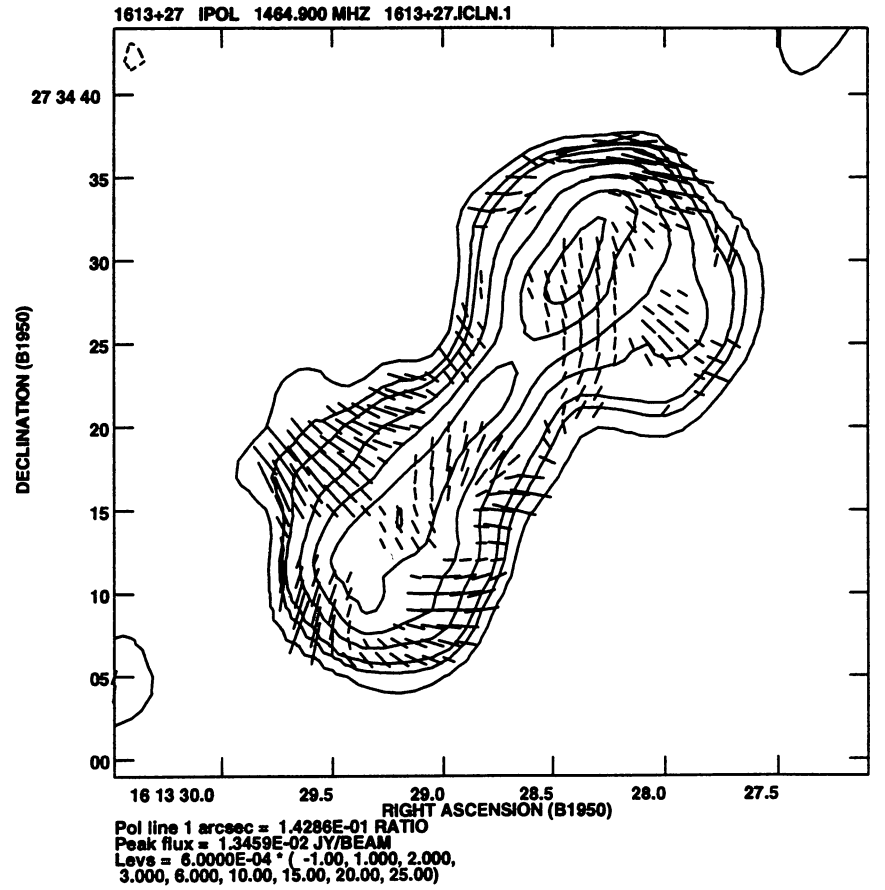


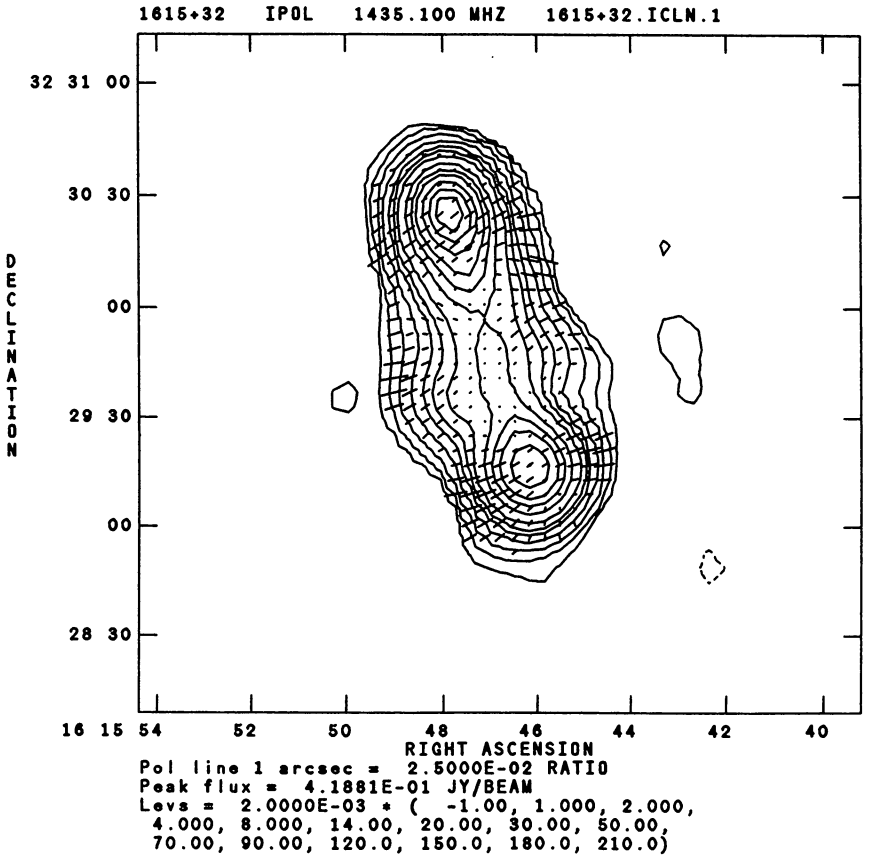


Fig. 1. continued

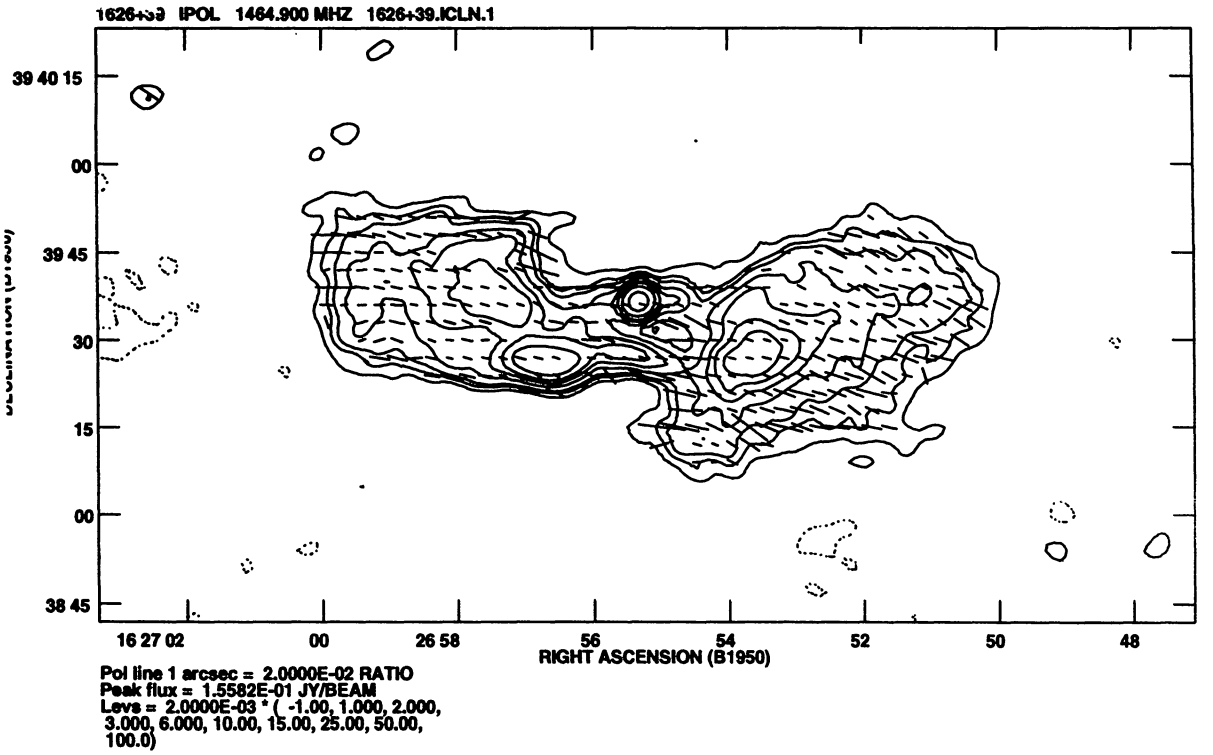


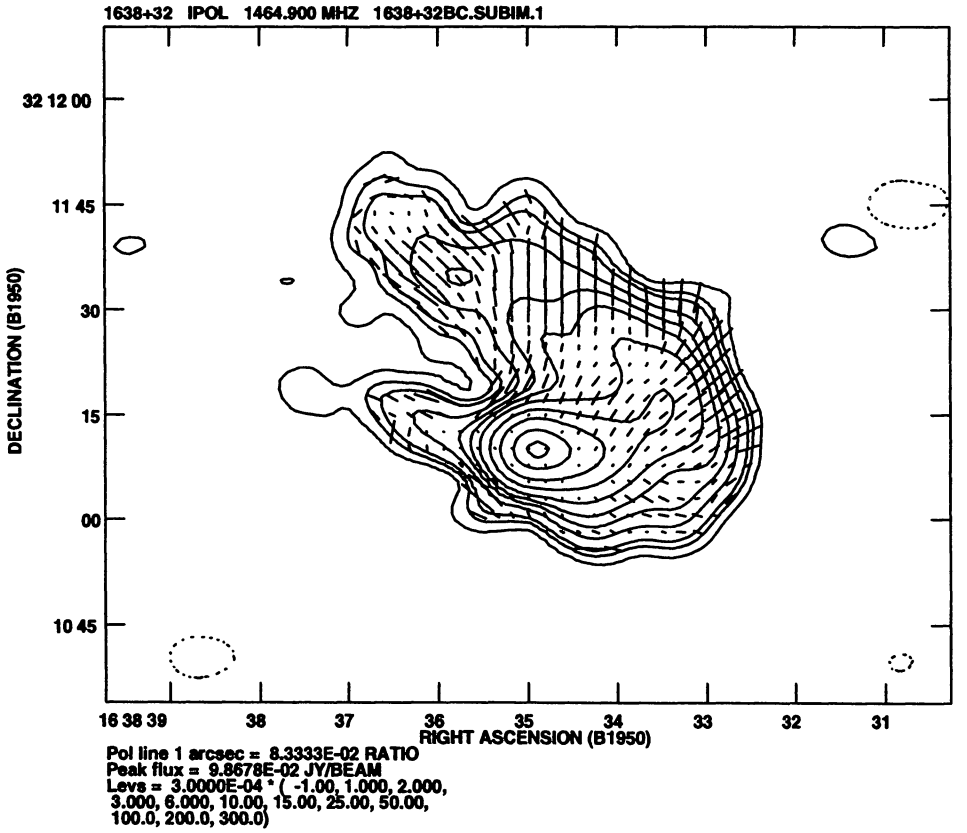


Fig. 1. continued

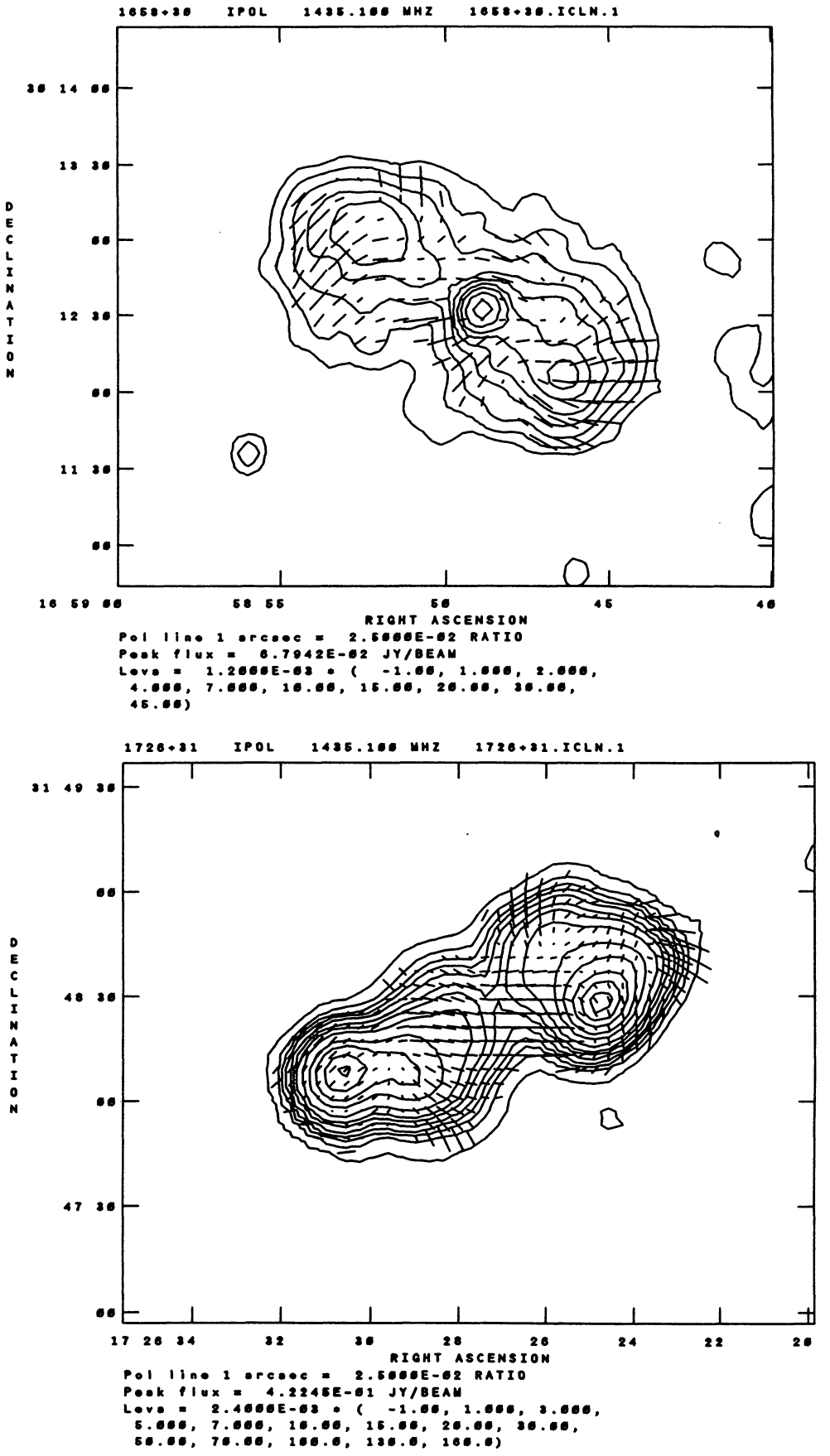


**Fig. 1.** continued

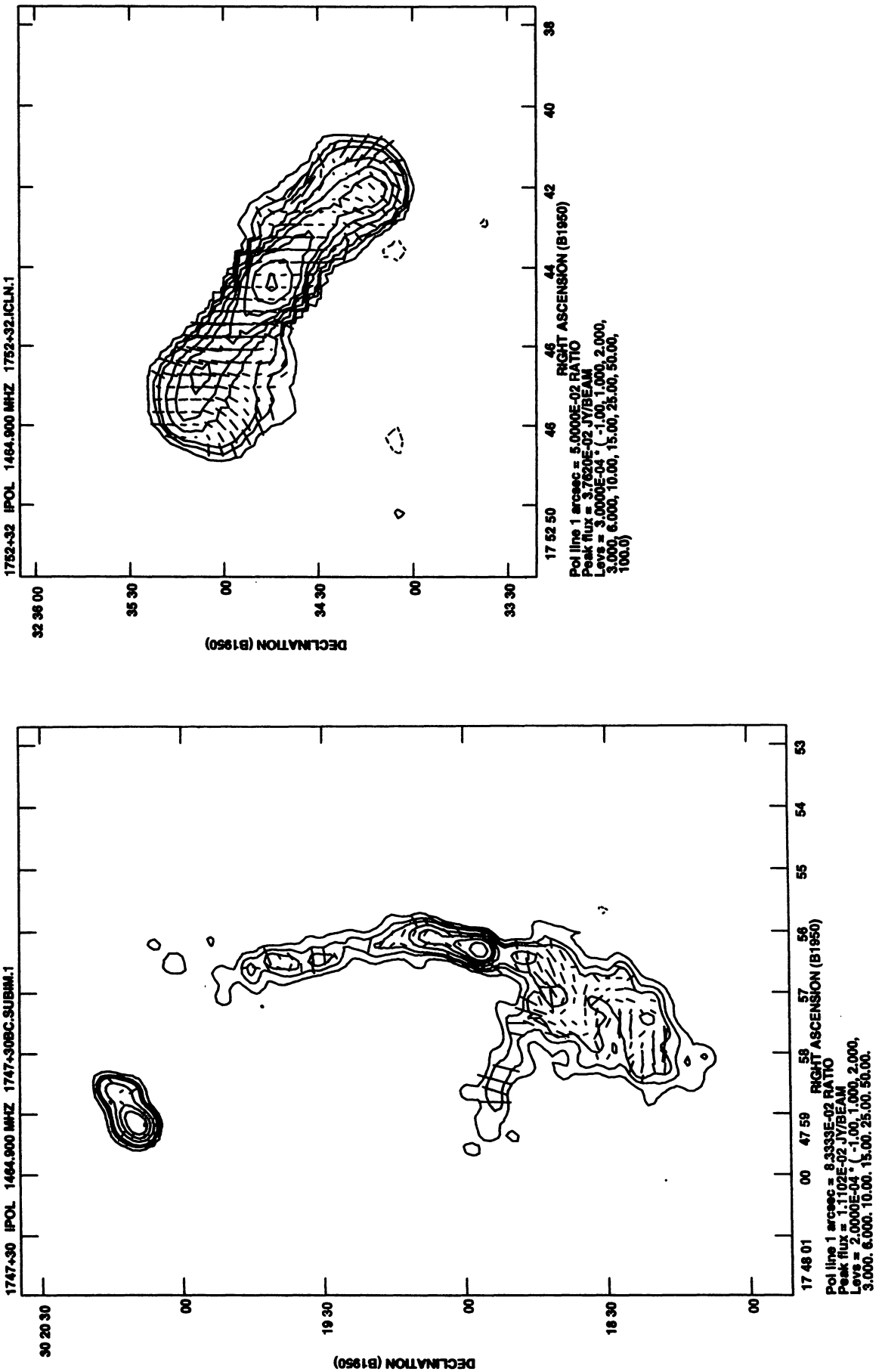


Fig. 1. continued

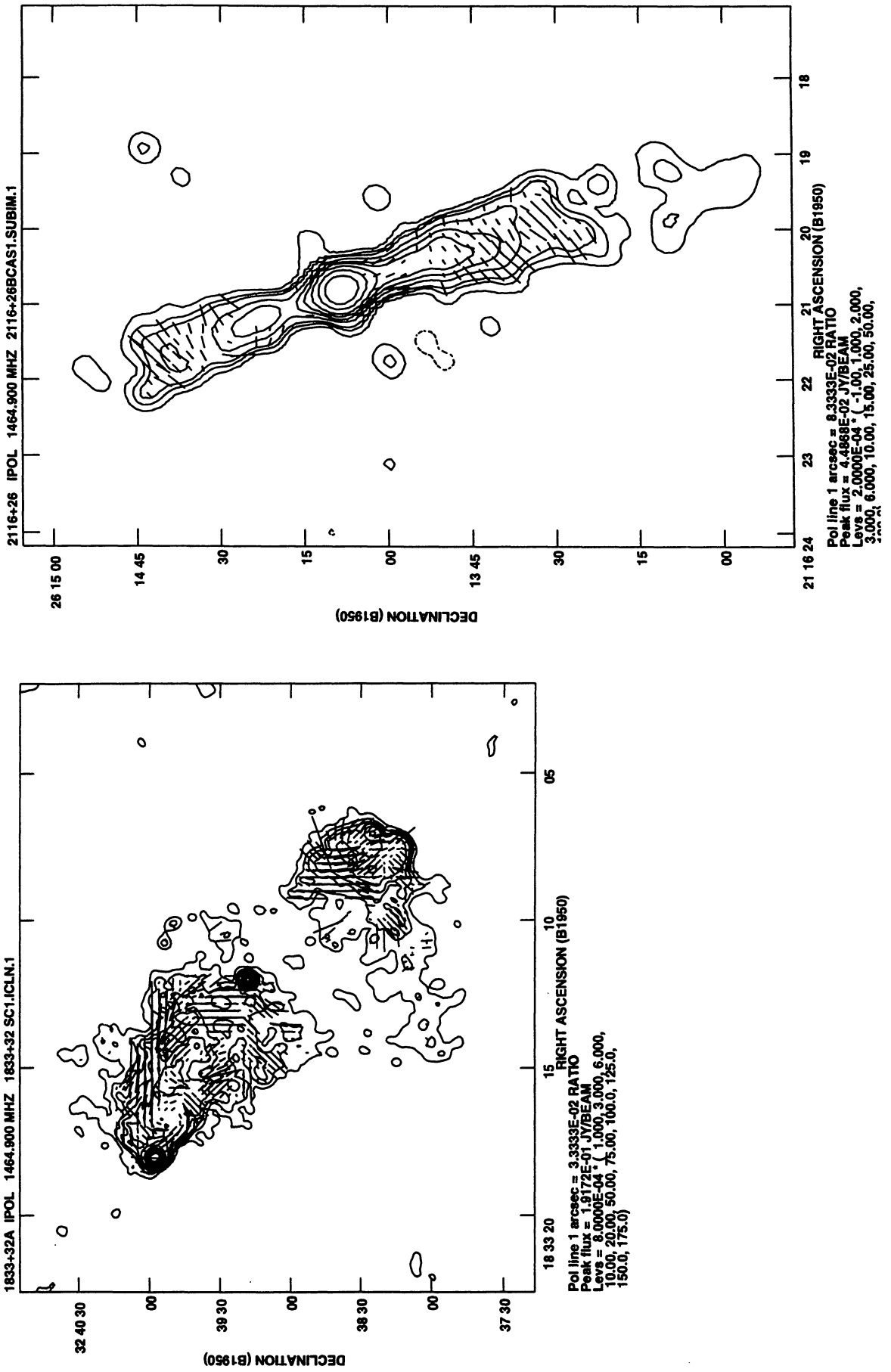


Fig. 1. continued

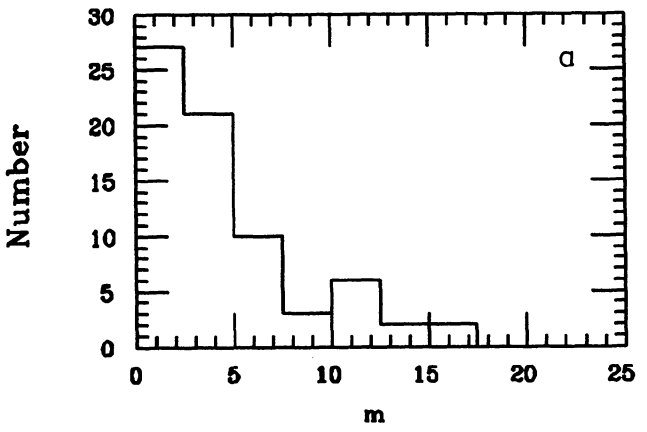


Figure 2a.

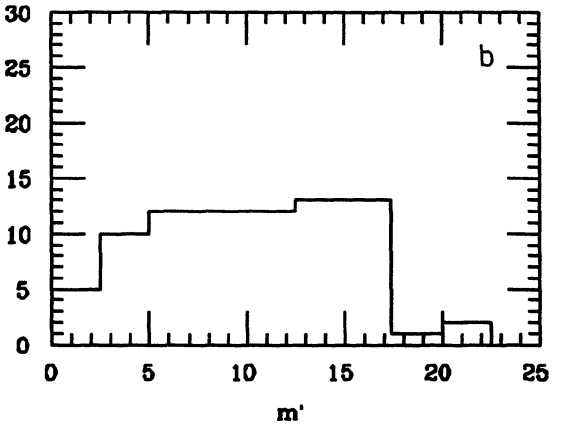


Figure 2b.

Fig. 2a and 2b. Distributions of $m$ and $m'$ integrated over each source

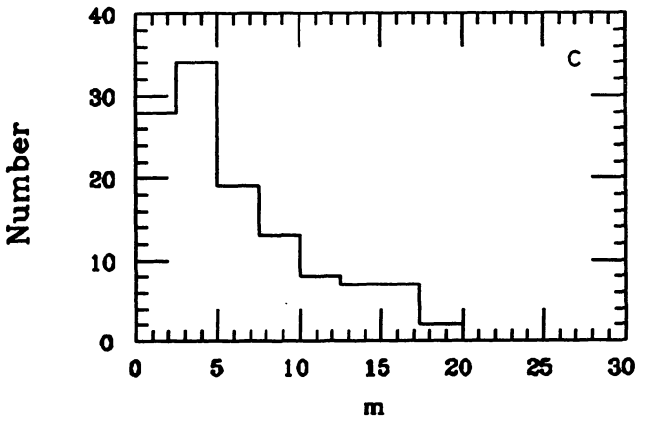


Figure 2c.

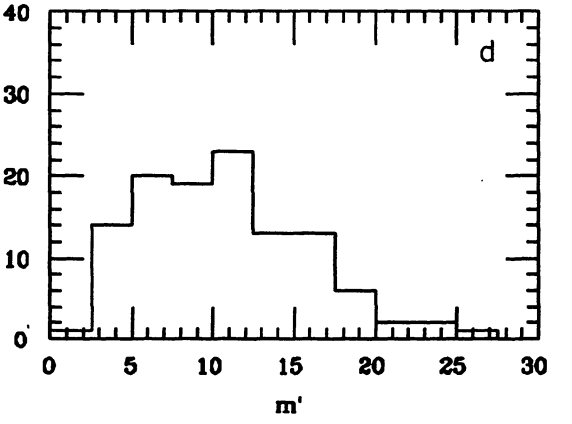


Figure 2d.

Fig. 2c and 2d. Distributions of $m$ and $m'$ of the lobes for the sources with a double lobed structure